Interference Management in MIMO Networks

A Thesis
Presented to
The Academic Faculty

by

Sudhanshu Gaur

In Partial Fulfillment
of the Requirements for the Degree
Doctor of Philosophy in Electrical and Computer Engineering

School of Electrical and Computer Engineering
Georgia Institute of Technology
August 2008

Interference Management in MIMO Networks

Approved by:

Professor Mary Ann Ingram, Advisor
School of Electrical and Computer Engineering
Georgia Institute of Technology

Professor Gregory Durgin
School of Electrical and Computer Engineering
Georgia Institute of Technology

Professor Raghupathy Sivakumar
School of Electrical and Computer Engineering
Georgia Institute of Technology

Professor Prasad Tetali
School of Mathematics
Georgia Institute of Technology

Professor Geoffrey Li
School of Electrical and Computer Engineering
Georgia Institute of Technology

Date Approved: April 2008

To the memory of my mother, Rama Gaur

ACKNOWLEDGEMENTS

I would like to express my deep gratitude to Prof. Mary Ann Ingram for her invaluable advice and encouragement at every step of my PhD program. Without her unfailing support, patience, and belief in me, this thesis would not have been possible. Her contribution to this thesis goes well beyond her role as an academic supervisor and includes constant support on a personal level without which this journey may never have been completed. And for this, I am truly grateful.

I also thank the members of my thesis committee, Prof. Raghupathy Sivakumar and Prof. Geoffrey Li for being on my thesis reading committee. Their encouragement and enlightening suggestions have greatly improved my research and this dissertation. I express my appreciation to Prof. Gregory Durgin and Prof. Prasad Tetali for being on my dissertation committee.

A big part of my PhD learning experience has been the interaction and collaboration with fellow students at Georgia Tech. I have had wonderful lab-mates at Smart Antenna Research Lab. In particular my discussions with Hemabh Shekhar, Vikram Anreddy, Jeng-Shiann Jiang, and Vijay Ganugapati have benefitted me a lot. I also thank great friends and former colleagues Shantidev Mohanty, Chirag Patel, Ghurumuruhan Ganesan, Arnab Choudhury, Rajesh Luharuka, and Manas Bajaj, for their everlasting friendship and support. In addition, I thank all my friends outside Georgia Tech including Jasvinder Singh, Gaurav Sinha, Bhupinder Sooch, Kameshwar Chandrasekar, Ramanathan Viswanathan, and so many others for making my life in US a pleasant experience.

And foremost, I offer my heartfelt thanks to my parents and my brothers Himanshu, Nalinaksh, and Abhishek, for their everlasting encouragement, faith, support

and love. Thank you for everything. To you, I dedicate this work.

TABLE OF CONTENTS

LIST OF FIGURES

ABBREVIATIONS

ABER	$\triangleq$	Average Bit Error Rate
AWGN	$\triangleq$	Additive White Gaussian Noise
BER	$\triangleq$	Bit-Error Rate
CDF	$\triangleq$	Cumulative Distribution Function
CL	$\triangleq$	Closed-Loop
CL-MIMO	$\triangleq$	Closed-Loop MIMO
CSI	$\triangleq$	Channel State Information
DOFs	$\triangleq$	Degrees Of Freedom
FEC	$\triangleq$	Forward Error Correction
IID	$\triangleq$	Independent and Identically Distributed
INR	$\triangleq$	Interference-to-Noise Ratio
LOS	$\triangleq$	Line-of-sight
MAC	$\triangleq$	Multiple-Access Control
MIMO	$\triangleq$	Multiple-Input Multiple-Output
MISO	$\triangleq$	Multiple-Input Single-Output
MMSE	$\triangleq$	Minimum Mean-Square Error
MSE	$\triangleq$	Mean Square Error
MUD	$\triangleq$	Multiuser Detection
NBS	$\triangleq$	Norm Based Selection
NLOS	$\triangleq$	Non-line-of-sight
OL	$\triangleq$	Open-Loop
OL-MIMO	$\triangleq$	Open-Loop MIMO
OSTBC	$\triangleq$	Orthogonal Space Time Block Code
PDF	$\triangleq$	Probability Density Function
RF	$\triangleq$	Radio Frequency

SDMA	$\triangleq$	Space Division Multiple Access
SIC	$\triangleq$	Successive Interference Cancellation
SISO	$\triangleq$	Single-Input Single-Output
SIMO	$\triangleq$	Single-Input Multiple-Output
SIR	$\triangleq$	Signal-to-Interference Ratio
SM	$\triangleq$	Spatial Multiplexing
SNR	$\triangleq$	Signal-to-Noise Ratio
STBC	$\triangleq$	Space Time Block Code
SVD	$\triangleq$	Singular-Value Decomposition
TDMA	$\triangleq$	Time-Division Multiple-Access
V-BLAST	$\triangleq$	Vertical - Bell Labs Layered Space-Time
WLAN	$\triangleq$	Wireless Local Area Network
ZF	$\triangleq$	Zero-Forcing

SUMMARY

New interests in wireless communications driven by consumer electronics have raised the bar in terms of throughput for wireless networks. Towards this goal, the multiple-input multiple-output (MIMO) systems have emerged as a key technology capable of delivering extremely high data rates. Extensive research in MIMO technology has led to its inclusion in several wireless standards including IEEE 802.11n (WLAN) and IEEE 802.16e/m (WiMax). The objective of the research presented in this dissertation is to develop efficient low complexity interference management techniques for improving the performance of MIMO networks.

The first half of this dissertation focuses on the interference problems arising in the context of space-division multiple access (SDMA) based MIMO networks, which more effectively exploit the available network resources than time-division multiple access (TDMA) MIMO networks. Sub-optimal techniques for joint optimization of co-channel MIMO links are considered by applying optimal antenna selection-aided stream control algorithms. These algorithms are tested on both simulated and measured indoor MIMO channels. It is shown that the use of the SDMA scheme along with partial channel state information (CSI) at the transmitters significantly reduces the signaling overhead with minimal loss in throughput performance. Next, a mean squared error (MSE) based antenna selection framework is presented for developing low complexity algorithms for finite complexity receivers operating in the presence of co-channel interference. These selection algorithms are shown to provide reasonable bit-error rate (BER) performance while keeping the overall system complexity low.

The later half of this dissertation considers interference problems for space-time encoded transmissions. Despite the low data rates supported by various Orthogonal

Space-Time Block Codes (OSTBCs), they are attractive from a network point of view as they cause correlated interference, which can be mitigated using only one additional antenna without sacrificing space-time diversity gains. These algebraic properties of linear OSTBCs are exploited to facilitate a single-stage and minimum MSE (MMSE) optimal detector for two co-channel users employing unity rate real and derived rate-1/2 complex OSTBCs for 3 and 4 transmit antennas. Furthermore, a single-stage multi-user interference suppression technique is proposed for OSTBC interference that exploits the temporal and spatial structure of OSTBCs leading to simple linear processing. Next, a sub-optimal space-time IC technique is developed for a V-BLAST link subjected to Alamouti interference. The proposed IC technique outperforms conventional IC techniques that do not take the structure of Alamouti interference into account.

This research deals with the challenges posed by co-channel interference in MIMO networks and provides practical means of managing interference at a marginal cost of system performance. The physical layer algorithms provide low complexity solutions for interference management in SDMA MIMO networks, which can be used for the design of next generation multiple access control (MAC) layers.

CHAPTER I

INTRODUCTION

The field of wireless communications has witnessed revolutionary developments in the past decade. Tremendous research in this area has made it more realistic for future generation wireless networks to match the data-rates of wired networks. The key driving force behind these developments is the multiple-input multiple-output (MIMO) technology, which has rapidly emerged as a reliable means of supporting extremely high data rates over wireless channels. As a result, MIMO has been adopted as the key PHY layer technology for the upcoming WLAN standard, IEEE 802.11n, which is expected to offer 600 Mbps PHY rate. In addition, MIMO has also been adopted in several other wireless standards including the WiMAX standard, IEEE 802.16, and next generation cellular networks such as UMTS.

Different from conventional links with single antenna transceivers, MIMO links employ multiple antennas at both ends. These antennas can be used to create multiple spatial channels in the same bandwidth by partitioning a high signal-to-noise ratio (SNR) channel into many low-SNR subchannels. Thus, a MIMO link can carry multiple data streams in parallel on the same frequency band, leading to increased spectral efficiency. As a result, in a rich scattering environment the capacity of a MIMO link scales linearly with the number of transmit and receive antennas [18, 49]. For this reason, MIMO transceivers are an obvious choice for next-generation wireless networks, including WLANs. Apart from offering extremely high spectral efficiencies, MIMO links also offer an attractive diversity/rate trade-off. The additional degrees of freedom (DOF) due to multiple antennas can be used to suppress interference and/or lend diversity gains to protect data streams against transmission errors [56]. This

flexibility due to multiple antennas, enables MIMO networks to tolerate co-channel transmissions leading to better resource utilization than a time-division multiple access (TDMA) scheme [14].

1.1 Motivation and Challenges

The multiple-access control (MAC) protocol used in current WLAN standards, including the developing IEEE 802.11n standard with enhancements for higher throughput, is based on the carrier sense multiple access/collision avoidance (CSMA/CA) protocol. As a result, simultaneous transmissions from two or more neighboring nodes that might cause interference to each other are not allowed. This leads to sub-optimal performance for networks comprising MIMO capable nodes [14].

With these networks as our motivating application, we develop sub-optimal physical layer techniques that allow interfering MIMO links to operate simultaneously and provide a reasonable performance/complexity tradeoff. These algorithms can be viewed as resource allocation methods which might be used in next generation MAC layer designs to improve network performance. In this dissertation, we focus on the following techniques:

- **Stream control with partial channel state information (CSI):** We propose an efficient stream control aided by optimal antenna selection for jointly optimizing the network throughput for open-loop MIMO (OL-MIMO) systems. The partial CSI at the transmitter is used to convey the subset of selected transmit antennas. Next, the usefulness of this scheme is shown in the context of finite complexity linear receivers.

- **Mean-squared error (MSE) optimal antenna selection:** Several greedy algorithms are developed to improve the error performance of linear receivers in presence of co-channel interference. These algorithms aim to minimize the MSE

associated with the linear receivers and provide a good performance/complexity trade-off.

- **Suppression of Space-time interference:** Exploiting the rich algebraic structure of orthogonal space-time block codes (OSTBC) interference, we show computationally efficient ways to detect two co-channel users employing the same rate-1/2 OSTBC codes. Furthermore, we present linear interference cancellation (IC) techniques for suppressing space-time interference.

An optimal transmission scheme for OL-MIMO systems in an interference-free zone is to put independent data streams with equal power into different antennas [18, 49]. However, in an interference-limited environment this may not be the best strategy as it is likely overload the receiver with more streams than available antenna elements. In such situations, network throughput may still be improved by MAC layer regulation of the co-channel transmissions.

A distributed stream control mechanism was proposed for space-division multiple access (SDMA) networks, which greatly improves the overall network throughput compared to a TDMA network [13, 14]. This stream control mechanism works best with the closed-loop MIMO (CL-MIMO) systems but the required overhead is significant, as the CSI for each pair of transmit-receive nodes has to be signaled back to the transmitters. In addition, the implementation of stream control for CL-SDMA is numerically intensive, involving matrix decompositions, thus real-time implementation would become a challenge with growing size of channel matrices. On the other hand, stream control for OL-SDMA has significantly less complexity but it performs significantly worse relative to CL-SDMA when the interference is strong [13, 14].

In this dissertation, we propose an efficient stream control strategy assisted by optimal antenna selection for jointly optimizing the network throughput for OL-MIMO where only limited CSI is available at the transmitter. We show that a middle-path

approach of having a limited-feedback channel (used to convey the optimal subset of selected transmit antennas) provides a good trade-off between the feedback signaling load and the network throughput performance. Our results, for both simulated and measured channels, show that the performance gap between CL- and OL-SDMA with limited feedback can be substantially abridged if optimal antenna selection is combined with stream control.

The main challenge in employing stream control with optimal antenna selection for OL-SDMA systems is the search of optimal subset of transmit antennas. A straightforward approach is to evaluate the cost function (e.g., capacity, bit error rate) over all possible antenna subsets. However, it quickly becomes computationally prohibitive with increasing number of available antenna combinations. For instance, choosing 8 antennas out of 16 available antennas requires 12,870 computations of the cost function to determine the optimal antenna subset.

Various suboptimal antenna selection schemes for MIMO systems have been studied in the recent literature. The most simple one is norm-based selection (NBS), which selects the receive (transmit) antennas corresponding to the rows (columns) of the channel matrix with the largest Euclidean norms [43, 19]. Indeed, the main drawback of NBS is that it may lead to much lower capacity in the presence of receive (transmit) correlation [19]. A better approach is to remove the antennas in a step-by-step method, which causes minimal degradation in the capacity [36]. However, this method still involves the complexity of matrix inversion, which is avoided by performing incremental antenna selection starting with a null set of selected antennas [22, 19].

Most of the above studies assume channel capacity as the cost function instead of the more practical mean-squared error (MSE) or bit-error rate (BER) metrics, which are dependent on the receiver complexity. In this dissertation, we develop an MSE-based antenna selection framework for both minimum MSE (MMSE) and zero

forcing (ZF) receivers assuming presence of co-channel interference. For either the transmitter or receiver, there are two sequential greedy algorithms, one that starts with a full set of antennas and decrements, and the other that starts with an empty set that increments. The choice of which is best depends on how many antennas will ultimately be selected. These presented algorithms have low implementation complexity while offering near optimal error performance.

Another part of this dissertation is devoted to space-time interference cancellation techniques and multi-user detection of co-channel users employing Orthogonal Space-Time Block codes (OSTBCs). Despite the low data rates supported by various OSTBCs, they are attractive from a network point of view as they cause correlated interference, which can be mitigated using only one additional antenna without sacrificing space-time diversity gains [37], [26]. A simple suboptimal 2-stage linear receive processor can achieve IC of two co-channel users employing any rate-1/2 complex STBC based on an orthogonal design while preserving the diversity gains [45].

We exploit special algebraic properties of linear OSTBCs to facilitate a single-stage and MMSE-optimal detector for two co-channel users employing unity rate real and derived rate-1/2 complex OSTBCs for 3 and 4 transmit antennas. Furthermore, we propose a single-stage multi-user interference suppression technique for OSTBC interference that exploits the temporal and spatial structure of OSTBCs leading to simple linear processing. The algorithm requires only one additional antenna to cancel co-channel OSTBC interference.

1.2 Dissertation Outline

The rest of the dissertation is organized as follows: Chapter 2 presents an overview of MIMO technology and related concepts followed by a brief discussion of the stream control concept for joint optimization of co-channel links. Chapter 3 proposes stream control aided with optimal selection for OL-MIMO systems in the context of SDMA

networks. In Chapter 4, the stream control concept is extended to include finite complexity linear receivers. Chapter 5 presents MSE optimal antenna selection framework for ZF/MMSE receivers. These algorithms can be applied to interference limited environments such as MIMO ad hoc networks to assist stream control algorithms. In Chapter 6, we turn our attention to simplified IC methods for OSTBC users employing rate-1/2 codes and present linear IC techniques for two co-channel OSTBC users. Chapter 7 considers the problem of Alamouti interference for a co-channel V-BLAST link and develops sub-optimal space-time IC techniques. Finally, in Chapter 8, we conclude by summarizing our research contributions and open areas of research in interference management in MIMO networks.

CHAPTER II

BACKGROUND

In this chapter, we provide an overview of MIMO communication systems along with a brief discussion on their use in ad hoc networks and related challenges. The first section introduces some key concepts of MIMO systems. The modeling of a MIMO link is considered along with brief discussions on the channel capacities of open-loop (OL) and closed-loop (CL) MIMO systems. The next section presents various transmissions techniques associated with MIMO links. In particular, system designs for Spatial Multiplexing (SM) and Space-Time Block Codes (STBC) are considered. The last section discusses the problem of interference in MIMO networks and presents stream control algorithms for the joint optimization of co-channel MIMO links.

2.1 MIMO Architecture

A MIMO system consists of multiple antennas at both ends of the link. The use of multiple antennas offers it $N_r \times N_t$ degrees of freedom (DOFs), where N_r and N_t denote receive and transmit antennas, respectively. Unlike single antenna transceiver systems, which are limited to a single degree of freedom, MIMO systems can exploit multiple DOFs to alter various aspects of the underlying communication link such as channel capacity, bit-error rate (BER), coverage, interference suppression etc. More specifically, at the receiver end, these DOFs can be used to provide power gain of N_r over white noise, null as many as $N_r - 1$ interfering streams, or receive up to N_r parallel data streams. Similarly, at the transmitter end these DOFs can be used to provide transmit diversity, high power gain by concentrating the transmission power in beams, to avoid transmitting interference to certain directions, or to transmit N_t streams in parallel.

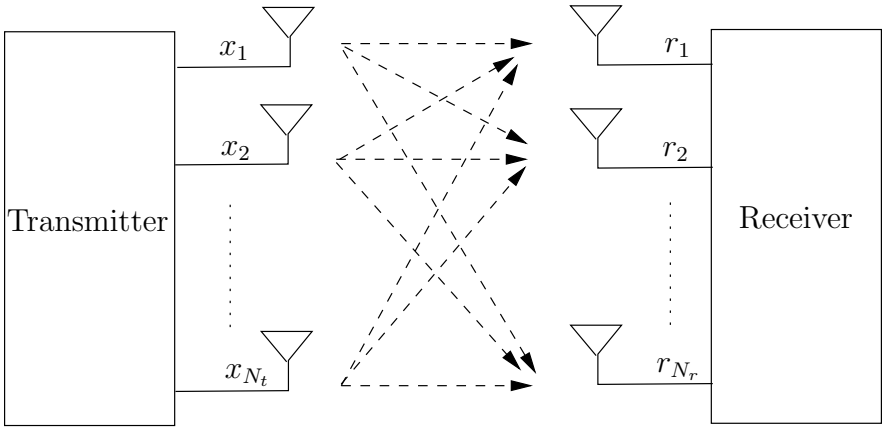

Figure 1: Block diagram of MIMO communication system

2.1.1 System Model

A generic MIMO communication system model is shown in Fig. 1. During each symbol period, N_t symbols are multiplexed for transmission over N_t transmit antennas. At the receiver, each antenna receives a linear combination of transmit symbols so that received baseband vector $\mathbf{r}$ is represented as

$$\mathbf{r} = \mathbf{H}\mathbf{x} + \mathbf{n} \tag{1}$$

where $\mathbf{H}$ denotes the $N_r \times N_t$ channel gain matrix whose $(i,j)^{th}$ element corresponds to the complex channel gain between i^{th} receiving antenna and j^{th} transmitting antenna, $\mathbf{x}$ is the transmit vector and $\mathbf{n}$ is the additive white Gaussian noise (AWGN) with variance $N_o/2$ per real and imaginary dimension. In this dissertation, the channel is assumed to be slowly varying, Rayleigh faded, and fixed for the duration of an entire burst. It is further assumed that

$$\mathrm{E}(\mathbf{x}\mathbf{x}^H) = \mathbf{P}; \quad \mathrm{E}(\mathbf{n}\mathbf{n}^H) = N_o\mathbf{I}; \quad \mathrm{E}(\mathbf{x}\mathbf{n}^H) = \mathbf{0} \tag{2}$$

where $\mathbf{P}$ is known as power allocation matrix, the subscript H denotes the conjugate transpose and $E(.)$ denotes the expected value of its argument.

At the receiver, the transmit vector can be estimated using well known linear

detectors such as ZF, or MMSE. In addition to ZF/MMSE solutions, more complex non-linear techniques such as successive interference cancellation (SIC) can be employed at the receiver to boost the BER performance.

2.1.2 Channel Capacity

A MIMO link is capable of creating multiple spatial channels to increase the data rate while maintaining reliable data detection at the receiver. Shannon's channel capacity, defined as the maximum rate of information that can be sent essentially error free across the channel, provides a useful measure of the data-carrying capability of MIMO systems. In an interference free environment, the channel capacity of the MIMO system can be expressed as

$$C = \max_{\mathbf{P}} \log_2 \left| \mathbf{I} + \frac{1}{N_o} \mathbf{HPH}^H \right|. \tag{3}$$

It is apparent that the channel capacity is dependent on the power allocation scheme at the transmitter and can be maximized if the transmitter is made aware of the underlying channel or it's statistics. To achieve this, the input symbols at the transmitter are passed through a linear precoder, which is optimized for given channel information available at the transmitter. Thus the received baseband vector after precoding can be represented as

$$\mathbf{r} = \mathbf{HFx} + \mathbf{n} \tag{4}$$

where $\mathbf{F}$ is the precoder matrix with complex elements. When the channel gain matrix is available at the receiver but not at the transmitter, as in OL-MIMO systems, the optimal precoder matrix $\mathbf{F} = \sqrt{P_T/N_t}\mathbf{I}$, where P_T denotes the total available transmit power. This leads to the best channel capacity for OL-MIMO systems given by [49, 18]:

$$C = \sum_{k=1}^{K} \log_2 \left(1 + \frac{P_T}{N_t} \sigma_k^2 \right) \tag{5}$$

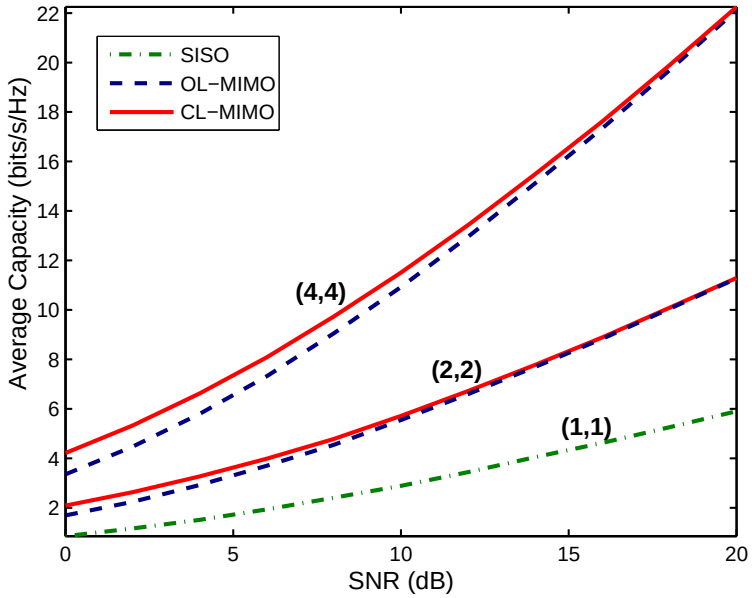

Figure 2: Capacity of SISO and (N_r, N_t) MIMO systems as a function of SNR, averaged over Rayleigh-faded channels

where σ_k, $k = 1, ...K$ denote the nonzero singular values (in decreasing order), which are obtained via the Singular Value Decomposition (SVD) of the channel matrix $\mathbf{H}$.

In CL-MIMO systems, the channel gain matrix is available both at the receiver and at the transmitter, thus allowing the link to decompose the channel into a logical collection of uncoupled parallel channels. In this case, the optimal precoder matrix can be obtained as $\mathbf{F} = \mathbf{V}\mathbf{\Phi}_F$. Here $\mathbf{\Phi}_F$ is a diagonal matrix whose k^{th} non-zero diagonal element is obtained using classical water-filling approach as [42]:

$$\alpha_k = \left[\left(\mu - \frac{1}{\sigma_k^2}\right)^+\right]^{\frac{1}{2}} \tag{6}$$

where $(.)^+$ indicates that only non-negative values are acceptable, and μ is chosen such that $\sum \alpha_k^2 = P_T$. Thus, the expression for the capacity for CL-MIMO systems becomes [49]

$$C = \sum_{k=1}^{K} \log_2(1 + \alpha_k^2 \sigma_k^2). \tag{7}$$

Next, in Figure 2 we compare the average capacities for single-input single-output

(SISO) and MIMO systems, where the average is taken over independent and identically distributed (i.i.d) Rayleigh fading channels. It is evident that OL/CL-MIMO systems offer far greater capacity than SISO over a wide range of SNR. Also, the capacity of MIMO system increases with increasing number of antennas. In fact, it is well known that a rich scattering environment leads to a linear increase in capacity with $\min(N_r, N_t)$ [18]. It is also apparent that the capacity gains offered by CL-MIMO systems over OL-MIMO systems are more prominent at low SNRs and diminishes rapidly as SNR improves [49, 18].

2.2 Transmission Strategies

Unlike SISO links, multiple antennas at the transmitter and receiver allow MIMO links to adapt transmissions to suite the link requirements such as increased spectral efficiency, transmit/receive diversity gains to reduce BER, improved range etc. This can be achieved by coding the signals across space and/or time using well known techniques such as Space-Time Coding, Spatial Multiplexing or Transmit Beamforming [1, 48, 52]. In this dissertation, we focus on two of the most common MIMO transmission strategies namely, Orthogonal Space-Time Block Codes (OSTBC) and Spatial Multiplexing (SM).

2.2.1 Orthogonal Space-Time Block Coding

Space-Time Block Codes (STBCs) are well known to provide transmit diversity without requiring explicit channel feedback from the receiver [1, 48]. The temporal and spatial structure of certain STBCs, called orthogonal STBCs (OSTBCs), offer additional advantage of maximum likelihood detection based only on linear processing at the receiver [48]. As a result, the OSTBCs are being widely adopted in various wireless communication standards such as the 3GPP cellular standard, WiMAX (IEEE 802.16), and IEEE 802.11n. An example of an OSTBC is the popular Alamouti code [1]

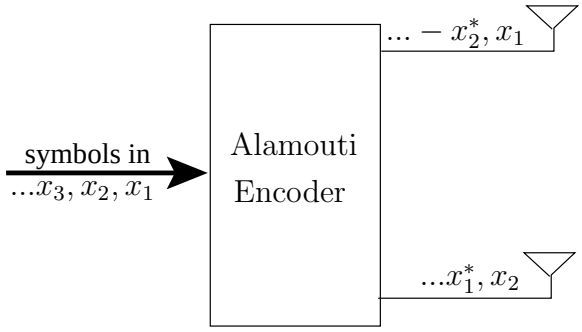

Figure 3: Alamouti space-time encoder [1]

$$\mathbf{X} = \begin{pmatrix} x_1 & -x_2^* \\ x_2 & x_1^* \end{pmatrix} \tag{8}$$

As shown in Figure 3, Alamouti's code encodes the input sequence of symbols across time and space. The Alamouti code falls into a more general category of linear STBC codes. These codes have relatively simple structure, as the transmitted code matrix, $\mathbf{X}$, is linear in the real and imaginary parts of the data symbols [32]:

$$\mathbf{X} = \sum_{i=1}^{N_s} x_i \mathbf{A}_i \tag{9}$$

where $\{x_i\}_{i=1}^{N_s}$ denotes the transmitted symbols and $\{\mathbf{A_i}\}_{i=1}^{N_s}$ are the $N_t \times N$ matrices representing the code structure, where N is the duration over which N_s symbols are transmitted using N_t antennas. From the definition of real orthogonal codes, it follows that

$$\mathbf{A}_i \mathbf{A}_j^T = \begin{cases} \mathbf{I}_N & \text{if } i = j \\ -\mathbf{A}_j \mathbf{A}_i^T & \text{otherwise} \end{cases} \tag{10}$$

For a MIMO link with N_t transmit antennas and N_r receive antennas, the received space-time signal $\mathbf{Y}$ corresponding to $\mathbf{X}$ can be written as [32]:

$$\mathbf{Y} = \mathbf{H}\mathbf{X} + \mathbf{V} \tag{11}$$

where $\mathbf{H}$ is the channel matrix and $\mathbf{V}$ denotes the complex additive white Gaussian noise matrix with zero mean and unity variance. For a quasi-static flat Rayleigh fading

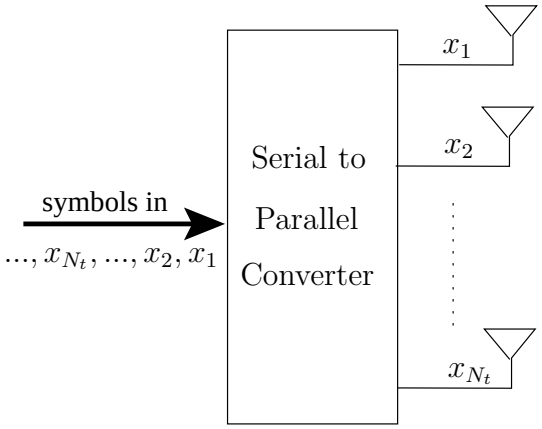

Figure 4: V-BLAST transmitter architecture [52]

channel, the received baseband signal can be represented using vector notation as [32]:

$$\mathbf{y} = \text{vec}(\mathbf{Y}) = \mathbf{F}\mathbf{x} + \mathbf{v} \tag{12}$$

where vec(.) denotes the standard vector representation of its argument, $\mathbf{v} = \text{vec}(\mathbf{V})$, and $\mathbf{F}$ is defined as

$$\mathbf{F} = \begin{pmatrix} \text{vec}(\mathbf{H}\mathbf{A}_1) & \dots & \text{vec}(\mathbf{H}\mathbf{A}_{N_s}) \end{pmatrix} \tag{13}$$

The vector representation for the received baseband signal in (12) can be expressed differently as $\mathbf{y}' = \mathbf{F}'\mathbf{x} + \mathbf{v}'$, where the operator $(.)'$ is defined as $\chi' = \begin{pmatrix} \text{Re}(\chi) \\ \text{Im}(\chi) \end{pmatrix}$. Therefore, the problem of detecting the transmitted data $\mathbf{x}$ given $\mathbf{y}$ amounts to minimizing the metric $||\mathbf{y}' - \mathbf{F}'\mathbf{x}||^2$. This can be solved using well known linear detection techniques such as MMSE or ZF filtering.

2.2.2 Spatial-Multiplexing

Different from OSTBC transmission techniques, Spatial Multiplexing schemes intend to increase the spectral efficiency of MIMO systems. Several SM-MIMO schemes have been developed including the most popular Vertical Bell Laboratories Layered Space Time (V-BLAST) architecture illustrated in Figure 3 [52]. In this dissertation, we will

focus on V-BLAST transmission for SM-MIMO systems, which requires transmission of N_t input symbols simultaneously via the N_t transmit antennas resulting in a much higher data rate, $N_s = N_t$. However, unlike OSTBC, the associated symbol detection using linear MMSE/ZF techniques is rather complex.

2.3 Optimization of Interference-Limited MIMO Links

As mentioned in the previous sections, MIMO links are better adept at suppressing interference compared to SISO links. In the following, we present a brief overview of capacity optimization techniques for interference limited MIMO networks.

2.3.1 Isolated Links

Many studies on MIMO systems consider a single point-to-point link or MIMO networks, which require links to access medium in a time-division fashion [18, 49, 10, 38]. Such communication systems avoid introducing co-channel interference. However, even then the links may still suffer from co-channel interference arising from other networks or jammers. For such networks, overall capacity optimization amounts to maximizing individual link capacities.

In the presence of strong interference, it is important not to overload the receivers. The optimal strategy for OL-MIMO systems is to excite as many as $N_r - N_{int}$ transmit antennas, where N_{int} denotes the number of incident interfering streams on the intended receiver [51]. The precoder matrix in this case is:

$$\mathbf{F}_i = \sqrt{\frac{P_T}{N_r - N_{int}}}\text{diag}\Big(\underbrace{1, 1, ..., 1}_{N_r - N_{int}}, \underbrace{0, 0, ..., 0}_{N_t - N_r + N_{int}}\Big) \tag{14}$$

where $diag(.)$ denotes the diagonal matrix formed by the elements of its vector argument.

For CL-MIMO systems, the water-filling approach in (6)-(7) can be modified to accommodate fixed non-white interference at the receiver of a link (represented by a

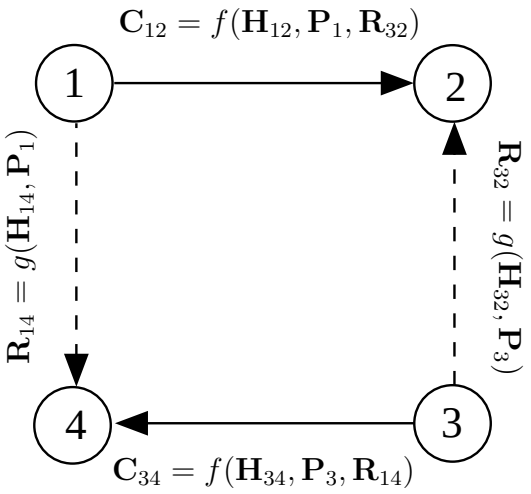

Figure 5: Mutually dependent link capacities and transmission strategies in a SDMA network.

noise-normalized covariance matrix, $\mathbf{R}$) by *whitening the channel matrix* first. Applying a spatial whitening transform to the channel yields

$$\widetilde{\mathbf{H}} = [\mathbf{I} + \mathbf{R}]^{-1/2}\,\mathbf{H} \tag{15}$$

which reduces the capacity relation to the simple form in (3), with a substitution of $\mathbf{H} \rightarrow \widetilde{\mathbf{H}}$ [5]. Thus, the capacity formula becomes

$$C = \max_{\mathbf{P}} \log_2 \left| \mathbf{I} + \widetilde{\mathbf{H}}\mathbf{P}\widetilde{\mathbf{H}}^H \right|. \tag{16}$$

The whitening operation assumes that the interfering symbols are unknown and only exploits the spatial characteristics of the interference. With the whitening transformation in (15)-(16), the optimum precoder becomes a function of the received interference, $\mathbf{R}$, in addition to the channel matrix, $\mathbf{H}$.

2.3.2 Co-channel Links

MIMO networks based on space-division multiple access (SDMA), which allow *controlled* co-channel transmissions, can outperform TDMA type networks [13, 14, 47]. Since these networks have multiple interfering links, the power allocation scheme, $\mathbf{P}_i$, used at each transmit node affects the interference correlation matrices, $\mathbf{R}_{ij}$, seen

by the receiver nodes. Therefore, optimization of individual link capacities does not necessarily translate to optimal network capacity as the link capacities have mutual dependence because the whitened channel matrix for a given link is a function of the interference. And the transmission strategy, in turn, is dependent on the whitened channel matrix. Thus, a change in the power allocation matrix of one link induces a change in the optimum power allocation matrix of the other co-channel links as shown in Figure 5.

As a result, the optimum precoder matrix and the powers of interfering CL-MIMO links cannot be calculated independently at each link and iterative methods are used instead [16, 8, 13, 14]. Joint transmit and receive beamforming for interfering SISO links is studied in [8], where the antenna weights and transmit powers are optimized to achieve certain SIRs for each link. An iterative stream control algorithm for CL-MIMO systems is proposed in [13, 14] to maximize the SDMA network throughput. At each iteration, all transmit-receive pairs optimize their link capacities under measured interference and allocated transmit powers. Each link's transmission strategy is determined according to the water-filling solution given in (16).

CHAPTER III

STREAM CONTROL WITH ANTENNA SELECTION

In the previous chapter, we highlighted the mutual dependence of optimal power allocation schemes for interfering MIMO links and the interference covariance matrices. In this chapter, we consider the joint optimization of these interfering MIMO links in the context of an SDMA network. Different from [13], we propose a low complexity stream control algorithm for OL-SDMA systems that provides a good tradeoff between feedback signaling load and the network throughput performance. The proposed algorithm augments stream control approach through the use of optimal antenna selection to jointly optimize the interfering links.

In the past, the joint optimization problem for interfering MIMO links has been treated by several researchers [16, 17, 7, 11, 12]. For cellular systems, iterative methods were used to optimize the uplink in [16] and the downlink in [17]. In [11] and [12], the authors explore ways to control the relative capacities of the interfering CL-MIMO links. In [11], each link iteratively maximizes the closed-loop capacity of its whitened channel under power constraints that generally differ among nodes, and in [12], each link minimizes the interference it makes on its neighbors, subject to capacity constraints. In [13], Demirkol et al. considered CL-MIMO systems and proposed a distributed stream control mechanism wherein an additional stream is added if it leads to an increment in the network throughput. The authors show that MIMO nodes operating under this strategy improve the overall network throughput compared to a TDMA protocol, in which MIMO links operate in succession.

Although stream control works best with CL-SDMA, the overhead is significant,

as the CSI for each pair of transmit-receive nodes has to be signaled back to the transmitters. Moreover, implementation of stream control for CL-SDMA is numerically intensive, involving matrix decompositions, thus real-time implementation would be a challenge as the channel matrix size grows. On the other hand, stream control for OL-SDMA has significantly less complexity. In [13], CL-SDMA was compared with OL-SDMA, where both used stream control, but the antenna selection in OL-SDMA was deterministic; in this case, OL-SDMA performed significantly worse relative to CL-SDMA when the interference was strong. In this chapter, we extend the analysis of [13] for OL- SDMA systems and show that a middle-path approach of having a limited feedback channel (used to convey the set of selected transmit antennas) provides a trade-off between the feedback signaling load and the network throughput performance.

In the next section, we outline the system model followed by a brief overview of optimal power allocation schemes for fixed interference. In the next two sections we discuss the simulation results and compare with the measured data. We show that for both simulated and measured channels, the performance gap between CL- and OL-SDMA with limited feedback can be substantially abridged if optimal antenna selection is used in addition to stream control.

3.1 System Model

Consider a simple network as shown in Figure 6, consisting of two spatial multiplexing MIMO links where each link is subjected to co-channel interference from the other link. The average signal-to-interference ratio (SIR) varies linearly as $10\log(R/D)^n$ on a logarithmic scale, where n denotes the path-loss exponent, R and D denote the receiver-transmitter separation for the interfering and the desired link, respectively.

The transmitting nodes are equipped with N_t antenna elements and receiver nodes use N_r antennas. Each transmitter uses a linear precoder to improve the system

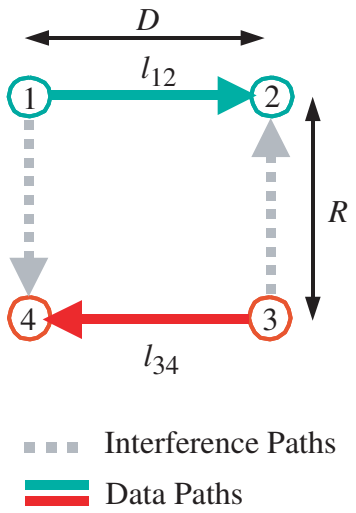

Figure 6: A simple 2-link network with spatial multiplexing transmissions.

performance. The received baseband vector corresponding to the i^{th} link can be represented as

$$\mathbf{r}_i = \mathbf{H}_{ii}\mathbf{F}_i\mathbf{x}_i + \mathbf{H}_{ji}\mathbf{F}_j\mathbf{x}_j + \mathbf{n} \tag{17}$$

where $\mathbf{H}_{ij}$ denotes the channel gain matrix corresponding to the transmitter of the j^{th} link and receiver of the i^{th} link, $\mathbf{F}_i$ is the precoder matrix with complex entries, $\mathbf{x}_i$ is the transmit vector corresponding to the i^{th} link and $\mathbf{n}$ is the additive white Gaussian noise (AWGN), having variance $N_o/2$ per real and imaginary dimension. The channel is assumed to be slowly varying, Rayleigh faded, and fixed for the duration of an entire burst. It is further assumed that

$$\mathrm{E}(\mathbf{n}\mathbf{n}^H) = N_o\mathbf{I}; \quad \mathrm{E}(\mathbf{x}_i\mathbf{n}^H) = \mathbf{0} \tag{18}$$

$$\mathrm{E}(\mathbf{x}_i\mathbf{x}_j^H) = \begin{cases} \mathbf{I} & \text{if } i = j \\ \mathbf{0} & \text{otherwise} \end{cases} \tag{19}$$

where the subscript H denotes the conjugate transpose and $E(.)$ denotes the expected value of its argument.

3.2 Capacity-Optimal Stream Control

In this section, we briefly discuss the optimal precoder and decoder design with respect to system throughput for OL- and CL-SDMA systems. Our goal is to maximize the network throughput, which is defined as the sum of the link data rates.

3.2.1 CL-SDMA System

The traditional water-filling approach can be modified to accommodate fixed non-white interference at the receiver of a link by whitening the channel matrix [5]:

$$\widetilde{\mathbf{H}}_{ii} = (N_o\mathbf{I} + \mathbf{H}_{ji}\mathbf{F}_j\mathbf{F}_j^H\mathbf{H}_{ji}^H)^{-\frac{1}{2}}\mathbf{H}_{ii} \tag{20}$$

Let the SVD of the whitened channel matrix be denoted as $\widetilde{\mathbf{H}}_{ii} = \mathbf{U}_i\mathbf{\Sigma}_i\mathbf{V}_i^H$. The optimal precoder matrix for the i^{th} link can be written as $\mathbf{F}_i = \mathbf{V}_i\mathbf{\Phi}_F$ where $\mathbf{\Phi}_F$ is a diagonal matrix whose k^{th} non-zero diagonal element is given by [42]:

$$\alpha_k = \left[\left(\mu - \frac{1}{\sigma_k^2}\right)^+\right]^{\frac{1}{2}} \tag{21}$$

where $(.)^+$ indicates that only non-negative values are acceptable, σ_k^2 denotes the SVD values of the whitened channel, P_T denotes the available transmit power, and μ is chosen such that $\sum \alpha_k^2 = P_T$. It may be noted that the capacity based precoder design is not necessarily optimal for finite complexity transceivers as will be explained in Chapter 4.

3.2.2 OL-SDMA System with Optimal Antenna Selection

For an OL-SDMA system, the best strategy is to allocate equal power to all transmit antennas [7]. In the presence of strong interference, not all transmit antennas are used, to avoid overloading the receiver. In this case, the optimal strategy is to excite as many as $N_r - N_{int}$ transmit antennas, where N_{int} denotes the number of incident interfering streams on the intended receiver [51]. The precoder matrix in this case is:

$$\mathbf{F}_i = \sqrt{\frac{P_T}{N_r - N_{int}}}\text{diag}\Big(perm\Big(\underbrace{1,1,...,1}_{N_r-N_{int}},\underbrace{0,0,...,0}_{N_t-N_r+N_{int}}\Big)\Big) \tag{22}$$

where $diag(.)$ denotes the diagonal matrix formed by the elements of its vector argument and $perm(.)$ denotes the permutation of the elements of the vector argument based on antenna subset selection.

3.3 Simulation Results

In this section, we present simulation results for 2-link network as shown in Figure 6 and the 3-link network. The results are generated using Monte Carlo simulation of 1000 channel trials. For the CL-SDMA results, the algorithm of [13] was used. In [13], authors demonstrate the usefulness of stream control for various SDMA techniques with the exception of OL-SDMA with optimal antenna selection. This section mainly considers SDMA schemes with stream control and draws performance comparisons between OL-SDMA performance with deterministic antenna selection and optimal antenna selection. For more detail about the contents of this section, with the exception of optimal selection, the reader is referred to [14]. We consider a fair energy transmission approach, which requires both TDMA and SDMA networks use equal transmit powers, to allow for a fair performance comparison. The noise-normalized transmit power is fixed at $P_T = 20$dB for the TDMA scheme. For SDMA scheme, the total transmit power is divided equally among all the transmitting nodes, i.e. $= P_T/2 = 17$dB for the 2-link network and $= P_T/3 = 15.2$dB for the 3-link network.

3.3.1 Throughput Performance

Figure 7 shows the average percent throughput improvements for several SDMA schemes relative to TDMA for a 2-link network. The horizontal axis is $n\log(R/D)$, where n is the path loss exponent. As a reference, the 802.11 MAC is likely to enforce time multiplexing due to interference if $R/D < 2$. For $n = 3$, for example, $R/D < 2$ corresponds to $3\log(R/D) < 0.9$. Therefore, if an SDMA scheme has positive throughput improvement for $n\log(R/D) < 0.9$, then a MAC that exploits SDMA, such as the one in [47], would outperform the 802.11 MAC.

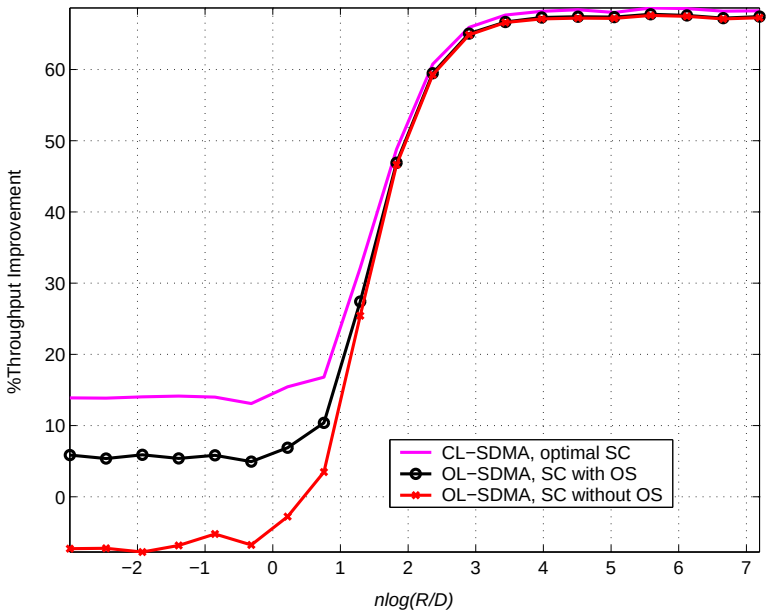

Figure 7: Average improvement in the network throughput relative to closed-loop TDMA, $(T - T_{\text{TDMA}}/T_{\text{TDMA}} \times 100\%$, fair energy approach. SC stands for stream control and OS stands for optimal antenna selection.

From Figure 7, we observe that CL-SDMA with stream control yields the best performance as expected. In [13], authors highlight the importance of stream control, which strikingly improves the throughput of OL-SDMA in strong interference regions. Yet, without optimal selection, stream control is not enough to make SDMA better than TDMA for $n \log(R/D) < 1/2$, when the interference is strong. However, when optimal antenna selection is used, the gap between CL-SDMA and OL-SDMA is reduced and in fact OL-SDMA outperforms TDMA even in high interference regions, offering an improvement of about 5%. For $n \log(R/D) > 1$, the interference from neighboring nodes is weak enough to allow the use of 4 data streams, thus explaining similar performances by various SDMA schemes. Thus stream control and optimal selection are the key factors in throughput performance when the interference is strong.

We also found that for a 3-link hexagonal network model, the average percent throughput improvement curves for different SDMA schemes follow similar trends.

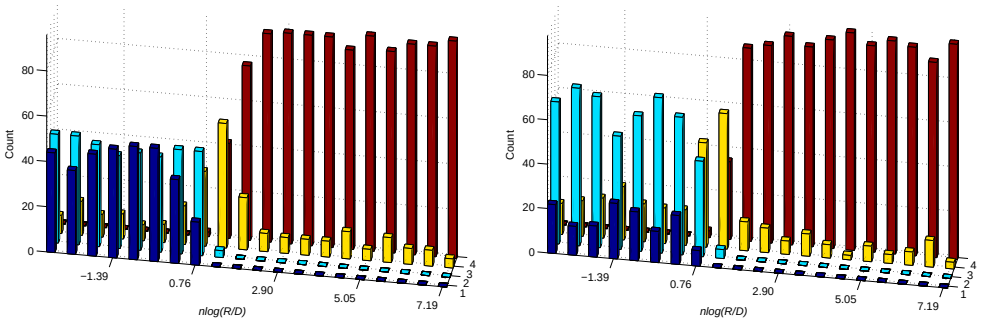

(a) OL-SDMA, SC with deterministic antenna selection

(b) OL-SDMA, SC with optimal antenna selection

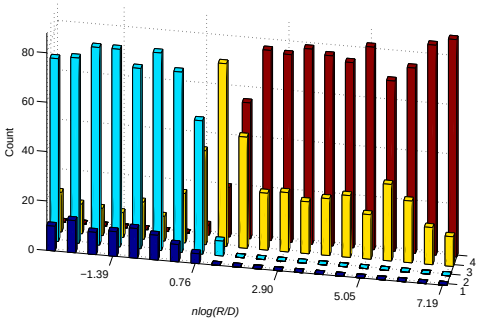

(c) CL-SDMA, SC

Figure 8: Histograms of number of streams used by one link with different MIMO configurations for different $n\log(R/D)$ values. Each layer of bars is associated with a different number of streams used, as indicated on the y-axis.

Again CL-SDMA with stream control yields the best performance with an improvement of about 20% over TDMA when the interference is strong. Also, OL-SDMA scheme with deterministic antenna selection performs poorly when $R \ll D$. With optimal antenna selection combined with stream control, OL-SDMA is able to provide an improvement of about 8% over TDMA. In the weak interference environment, all SDMA schemes exhibit superior performances against TDMA scheme with an improvement of about 122%.

3.3.2 Number of Streams and Stream Control

We shall consider the previous 2-link topology, assuming the noise-normalized total transmit power of each link is set to 17dB, and each node is assumed to have 4 antennas. 100 channel trials are generated, and the link parameters are found using the stream control method for 20 different values of $n\log(R/D)$. Figure 8 demonstrates the regulation of streams by different SDMA schemes as a function of the strength of interference, which varies with $n\log(R/D)$. We observe that, in accordance with [6], all the SDMA schemes mostly use 4 streams when interference is weak, thus greatly improving the throughput of the network. However, the similarity ends when the interference is significant ($R \ll D$). Figure 8(a) shows histograms of the number of streams used by link l_{12} with OL-SDMA with stream control but with deterministic antenna selection. It is apparent that when interference is strong, the link mostly uses either one or two streams with about equal probability. Figure 8(b) shows that with optimal antenna selection, OL-SDMA mostly uses 2 streams when the interference is strong. This is because if both the links use single stream, it would leave the victim receiver with two additional degrees of freedom, thus allowing each link to add another stream. It is apparent that optimal antenna selection-aided stream control enables OL-SDMA to exploit spatial multiplexing better than the deterministic selection. The transition occurs when $n\log(R/D) \approx 0.9$ when both the schemes use mostly three streams. It is interesting to note that after this transition, both schemes perform almost identically. Finally, Figure 8(c) shows the optimal stream control that could be achieved by CL-SDMA, the trends being very similar to those of [13]. Unlike OL-SDMA, with and without optimal antenna selection, CL-SDMA more often uses three streams when interference is relatively weak. Comparing different schemes, we see that optimal stream control, in consonance with [6] and [51], eliminates the use of excessive numbers of streams when interference is strong. In particular, the algorithm penalizes additional streams for $n\log(R/D) < 0.76$. However,

when $n \log(R/D)$ exceeds 0.9, stream control has less influence.

3.3.3 Effect of Path-Loss Exponent

The average SIR varies as on the logarithmic scale, where n denotes the path-loss exponent. Therefore, a change in path-loss exponent value reflects as a change in the received SIR at a given (R/D) location. Thus the value of n actually determines the transition region from strong interference to weak interference. A change in the value of n shifts this transition point (R/D) without affecting stream control before or after the transition point.

3.4 Performance Over the Measured Channel

The experiments were conducted with our 3D MIMO measurement system at 5.8 GHz [28] in the Residential Laboratory (RL) at the Georgia Institute of Technology. As shown in Figure 9, there are two receive array (Rx) locations and eight transmit array (Tx) locations. For each Tx-Rx pair, measurements were sequentially performed to acquire the channel matrices for antenna spacing of 0.5λ , where λ is the wavelength. The matrices were measured at 51 frequencies (10MHz separation) to obtain $20 \times 51 = 1020$ realizations of (4,4) flat fading channel matrices. Four representative configurations will be considered Conf. I: (T2-R1, T7-R2), Conf. II: (T8-R1, T6-R2), Conf. III: (T3-R1, T4-R2), and Conf. IV: (T3-R1, T5-R2). The first two configurations represent channels with less correlated interference because the directions of data and interference paths are angularly separated for both links. For the last two configurations, the data and interference for both links are spatially more correlated because of the confinement of the hallway. In order to clearly illustrate the correlation between the links, the first and third configurations are shown in Figure 9 with solid and dashed arrows, respectively. All four links (data and interferences) are individually normalized such that the signal links have the same SNR, and the SIR is equal to 1. This approach maintains the angular spread of the multipaths, while

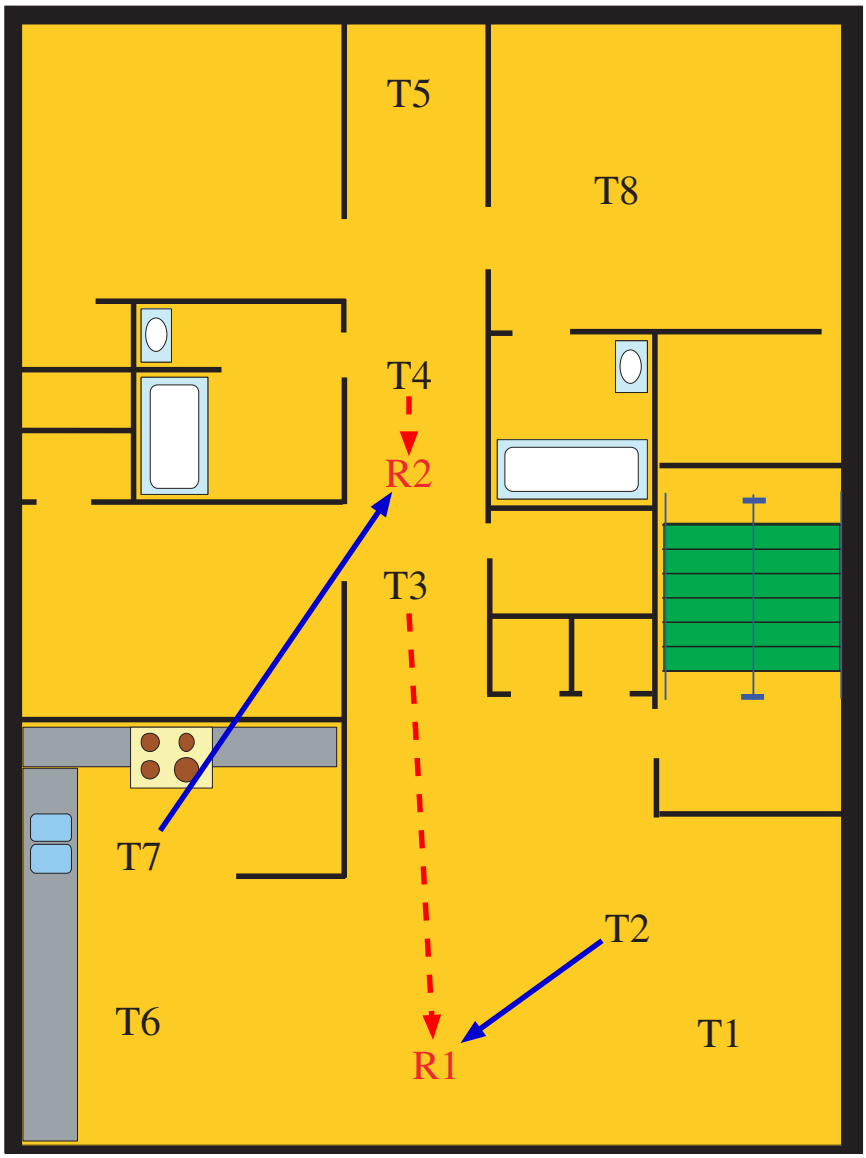

Figure 9: Layout of Residential Laboratory [28]

removing the range-dependent effects [28].

Figure 10 illustrates the average throughput performance of different MIMO schemes with stream control for different network configurations. As expected, CL-SDMA with stream control provides the best throughput performance for all four network configurations. Next we note that OL-SDMA with deterministic antenna selection yields better performance than OL-TDMA for Confs. I and II, when interference is less correlated. However, for highly correlated interference, as in Confs. III and IV,

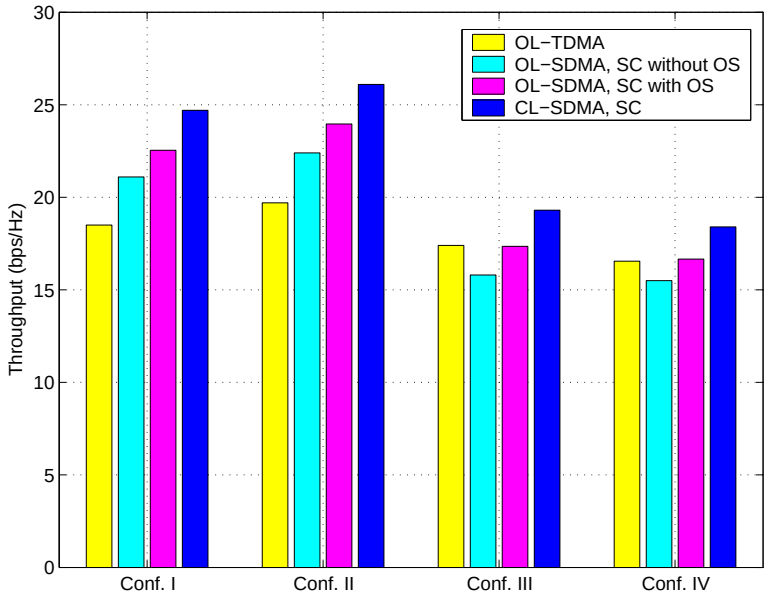

Figure 10: Average throughputs of various SDMA schemes for various network configurations. Equal-SNR normalization is assumed with SNR corresponding to 20dB noise-normalized total transmit power for TDMA and 17dB for schemes with interference

the performance of OL-SDMA without optimal selection degrades and is inferior to OL-TDMA. In fact, the throughput performance for all schemes goes down for Confs III and IV, when interference is highly correlated. This is because the correlated interference reduces the rank of the whitened channel matrix (19), thereby decreasing the system capacity. Hence for highly correlated interference, antenna selection becomes even more critical. From Figure 10, we observe that with optimal antenna selection, the performance of OL-SDMA improves significantly for all four configurations. However, OL-SDMA with optimal selection gives only comparable performance to OL-TDMA when the interference is highly correlated. Since OL-SDMA with optimal selection requires some CSI feedback, and TDMA requires none, TDMA is preferable in the correlated interference environment. In the other environments, however OL-SDMA with optimal selection offers an attractive alternative to TDMA.

3.5 Summary

In this chapter, we have analyzed the performance gains offered by the use of optimal transmit antenna selection in conjunction with stream control algorithm for OL-MIMO for both simulated data and measured data. Although CL-MIMO with stream control offers the best throughput, it has substantial overhead of providing the CSI to the transmit nodes. Our results for two- and three-link network models indicate that OL-MIMO with optimal antenna selection is an attractive alternative to CL-MIMO with stream control as it incurs a minimal overhead of specifying the chosen antenna set.

CHAPTER IV

STREAM CONTROL FOR FINITE COMPLEXITY RECEIVERS

In the previous chapter, we analyzed the capacity improvements offered by the use of optimal transmit antenna selection assisted stream control for OL-MIMO systems. The analysis presented therein along with the related work in [7, 11, 12, 13] is of theoretical importance as it evaluates the network performance in terms of Shannon's capacity assuming Gaussian inputs. However, in practice, discrete signalling constellations are used and transceiver complexity is also rather limited. In this chapter, we extend the analysis presented in the previous chapter along with the work in [13] to investigate the impact of stream control on the performance of interfering MIMO links assuming M-QAM constellations and linear MMSE receiver processing.

In the following sections, we first review the rate adaptation techniques for MIMO links given M-QAM constellations. Next, we present the simulation results for various SDMA configurations. Our simulation results indiciate a similar trend in throughput performances of CL- and OL-SDMA systems, as expected. Also, the use of optimal antenna selection in conjunction with stream control is shown to be beneficial for OL-SDMA systems with limited feedback.

4.1 System Design

In this section, we briefly discuss the optimal decoder design with respect to system throughputs for OL- and CL-SDMA systems. We again refer to the network shown in Figure 6, consisting of two SM-MIMO links where each link is subjected to co-channel interference from the other link. Our goal is to maximize the network throughput, which is defined as the sum of the link data rates.

4.1.1 Linear MMSE Decoder

Without loss of generality, let us consider the link l_{12}. To keep the analysis general, let us drop the link specific subscripts. The symbol estimation error vector associated with a linear decoder $\mathbf{C}$ can be written as $\mathbf{e} = \mathbf{x} - \mathbf{C}\mathbf{r}$, where $\mathbf{x}$ and $\mathbf{r}$ denote the transmit vector and received baseband vectors, respectively. The MMSE decoder requires that $\mathbf{C}$ be chosen such that the mean-squared error (MSE), $\mathrm{E}(||\mathbf{e}||^2)$, is minimized. The MSE can also be expressed as $\mathrm{tr}(\mathbf{R_e})$, where $\mathbf{R_e}$ is the error covariance matrix and tr(.) denotes the trace of its argument. Using simple matrix manipulations, $\mathbf{R_e}$ can be rewritten as,

$$\begin{aligned} \mathbf{R_e} &= (\mathbf{C} - \mathbf{F}^H\mathbf{H}^H{\mathbf{R_r}}^{-1})\mathbf{R_r}(\mathbf{C} - \mathbf{F}^H\mathbf{H}^H{\mathbf{R_r}}^{-1})^H \\ &\quad + \mathbf{I} - \mathbf{F}^H\mathbf{H}^H{\mathbf{R_r}}^{-1}\mathbf{H}\mathbf{F} \end{aligned} \tag{23}$$

where $\mathbf{R_r}$ is the receive covariance matrix. It is not difficult to show that the first term in (23) has non-negative diagonal entries. The MMSE solution, therefore, minimizes the contribution of the first term towards the MSE by choosing $\mathbf{C} = \mathbf{F}^H\mathbf{H}^H{\mathbf{R_r}}^{-1}$. Thus, the MSE for the i^{th} data stream is given by

$$mse_i = (\mathbf{I} - \mathbf{F}^H\mathbf{H}^H{\mathbf{R_r}}^{-1}\mathbf{H}\mathbf{F})_{ii} \tag{24}$$

where $(.)_{ii}$ denotes the i^{th} diagonal entry of its matrix argument. Now, the post-processing signal to interference and noise ratio (SINR) for the i^{th} data stream can be obtained as $sinr_i = \frac{1}{mse_i} - 1$, [42]. The data carrying capability of the link depends on this value of SINR.

4.1.2 Rate Adaptation

In this subsection, we give a brief overview of rate adaptation techniques for interfering MIMO links. We consider square as well as rectangular M-QAM modulations. The probability of bit error for the i^{th} data stream modulated using $I \times J$ rectangular

QAM can be linked to the SINR in (24) as [9]:

$$P_b(I,J) = \frac{1}{\log_2(I.J)}\left(\sum_{k=1}^{\log_2 I}\Psi_{I,J}(k) + \sum_{l=1}^{\log_2 J}\Psi_{J,I}(l)\right) \tag{25}$$

where the function $\Psi_{P,Q}$ can be computed as

$$\begin{aligned}\Psi_{P,Q}(n) &= \frac{1}{P}\sum_{j=0}^{P(1-2^{-n})-1}(-1)^{\lfloor m\rfloor}\left(2^{n-1} - \lfloor m+0.5\rfloor\right) \\ &\quad \times \mathrm{erfc}\left((2j+1)\sqrt{\frac{3\log_2(P.Q.sinr)}{P^2+Q^2-2}}\right)\end{aligned} \tag{26}$$

where $m = \frac{j.2^{n-1}}{P}$ and $\lfloor . \rfloor$ returns the greatest integer less than or equal to the argument. Now, the maximum rate supported by the i^{th} data stream with SINR $= sinr_i$ can be determined as

$$R_i = \log_2(I_i \times J_i), \tag{27}$$

where $\{I_i, J_i\}$ are chosen such that $M_i = I_i \times J_i$ is the largest constellation, which meets the target BER requirement. In the stream control algorithm, we use the rate expression in (27) instead of Shannon's capacity to compute the link throughputs. The maximum possible link rate R_i is a *stair-case* function of the associated SINR and target BER. It is apparent that the MMSE decoder doesn't necessarily optimize the link throughput as it tries to minimize the sum $\sum \frac{1}{sinr_i}$ instead of maximizing the sum $\sum R_i$.

4.2 Simulation Results

In this section, we present throughput results for the 2-link network shown in Figure 6. We consider several SDMA schemes with optional features such as stream control, optimal selection, channel whitening and draw performance comparisons among them and CL-TDMA scheme. In [13], the authors demonstrated the usefulness of stream control for various SDMA techniques, and in the previous chapter we further demonstrated the effectiveness of optimal selection-aided stream control for OL-SDMA; both

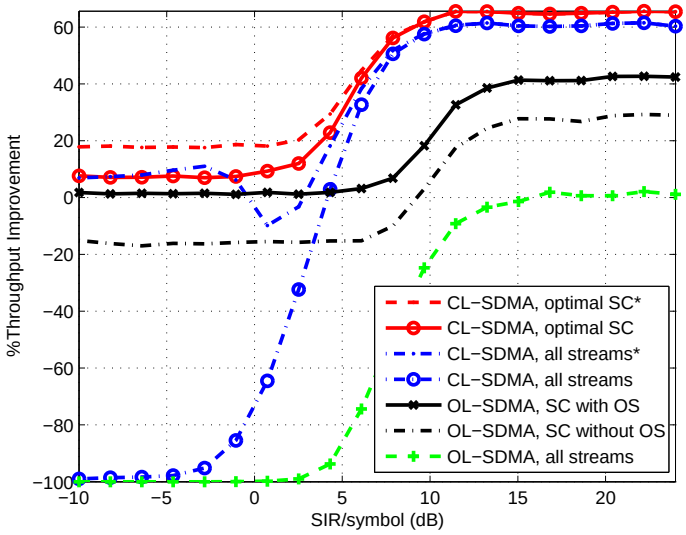

Figure 11: Average improvement in the network throughput relative to CL-TDMA for Average BER $= 10^{-2}$. SC stands for stream control and OS stands for optimal antenna selection. The subscript ()* indicates that whitened channel information is available at the transmitter.

using channel capacity metric to quantify the network throughputs. In this section, different from the past work, we assume linear MMSE receiver processing and evaluate the network throughput performance using the input signals drawn from both square and rectangular M-QAM constellations.

Each node is assumed to have 4 transmit/receive antennas. The results are generated using Monte Carlo simulation of 1000 channel trials. For the CL- and OL-SDMA results, the algorithm of [13] is used with one exception of using rate expression in (27) for computing link capacities. We consider a fair energy transmission approach, which requires both TDMA and SDMA networks use equal transmit powers, to allow for a fair performance comparison. The noise-normalized transmit power is fixed at $P_T = 20$dB for the TDMA scheme. For SDMA scheme, the total transmit power is divided equally among all the transmitting nodes, i.e. $\acute{P}_T = P_T/2 = 17$dB for the 2-link network.

4.2.1 Throughput Performance

Figure 11 shows the average percent throughput improvements of several SDMA schemes relative to CL-TDMA as a function of SIR with a target average BER = 10^{-2}. It is apparent that CL-SDMA with stream control yields the best performance as expected. For example, when the interference is strong (SIR $<$ 9dB), CL-SDMA with stream control using the whitened channel information, offers an improvement of about 18% over CL-TDMA. This gain can be explained as resulting from multiuser diversity because joint-optimization with stream control offers 8 channel modes to choose from rather than just 4 as in CL-TDMA. On the other hand, OL-SDMA without stream control gives extremely poor performance. This can be attributed to the fact that a linear decoder like MMSE is overwhelmed with interfering streams in the absence of stream control mechanism. When stream control is used with deterministic antenna selection, the performance of OL-SDMA is significantly improved but is still worse than that of CL-TDMA. However, optimal antenna selection-aided stream control improves the throughput of OL-SDMA by almost 18%, enabling it to match the performance of CL-TDMA. Thus OL-SDMA systems using a limited amount of feedback information offers an attractive alternative to CL-TDMA systems, which have significant signaling overhead. From Figure 11, we also observe that as the interference becomes weak, the performance of all SDMA schemes, barring OL-SDMA without stream control, observes significant improvement over CL-TDMA. We also note that the significance of whitened channel information at the transmitter reduces with reducing interference strength, as expected. It is also interesting to note that, contrary to the capacity results of [13], there is substantial gap between several SDMA schemes even in the high SIR zone.

Figure 12 shows the SDMA throughput improvements for a network with which permits far less packet errors, with average BER = 10^{-5}. The throughput curves for various SDMA schemes follow similar trends as in Figure 11. However, it can be seen

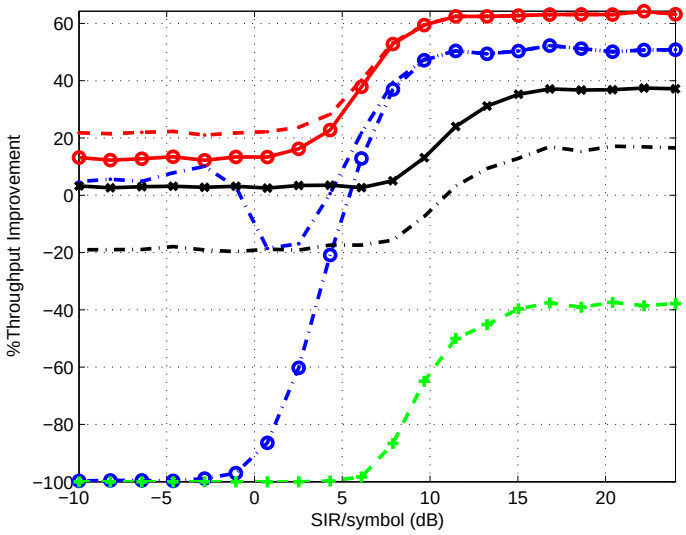

Figure 12: Average improvement in the network throughput relative to CL-TDMA for Average BER = 10^{-5}. The legend is same as in Figure 11.

that optimal antenna selection and stream control further improve the throughput performance of various SDMA schemes. On one hand CL-SDMA without stream control observes a fall in throughput, on the other hand CL-SDMA with stream control observes a further gain relative to CL-TDMA, which now amounts to about 21%. For OL-SDMA, the gain due to optimal antenna selection-aided stream control further increases to about 3% in the high interference zone. It can also be observed that OL-SDMA systems without stream control always perform worse than CL-TDMA systems even when interference is negligible.

Figure 13 shows the achievable bit rates for different MIMO schemes employing an MMSE decoder as a function of target BER for fixed SIR = 0dB. The performance curves for CL-SDMA with stream control using whitened channel information and OL-TDMA form the upper and lower bounds, respectively. The CL-SDMA scheme with stream control offers a gain of about 2.5 bps/Hz relative to CL-TDMA over a wide range of target BER. The availability of whitened channel information improves the performance of stream control, rendering a gain of about 1.25 bps/Hz. It is

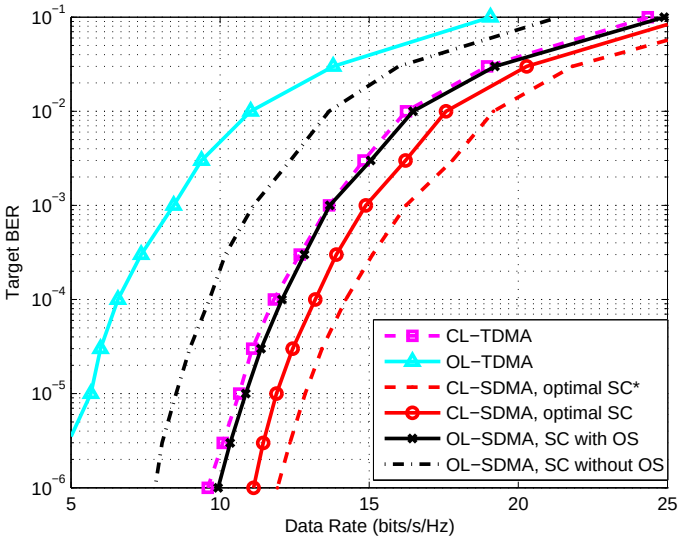

Figure 13: Achievable bit rates for various MIMO schemes as a function of target BER for SIR = 0dB. The subscript ()* indicates that whitened channel information is available at the transmitter.

interesting to note that the relative gap between any two MIMO schemes is almost independent of the target BER. From Figure 13, we also observe that optimal selection for OL-SDMA with stream control improves its performance by about 2.5 bps/Hz relative to deterministic selection. Infact, OL-SDMA with optimal selection, which requires a limited-feedback channel, matches the performance of CL-TDMA, which requires full CSI at the transmitter. Thus, it can be concluded that stream control along with optimal selection achieves a good tradeoff between performance required and feedback overhead.

4.2.2 Number of Streams and Stream Control

Figure 14 illustrates the regulation of streams by different SDMA schemes as a function of SIR, assuming a target BER = 10^{-5}. A hundred channel trials are generated, and the link parameters are found using the stream control method. Figure 14(a) shows the relative frequency of the number of streams used by link l_{12} for OL-SDMA with stream control but deterministic antenna selection. It is apparent that when

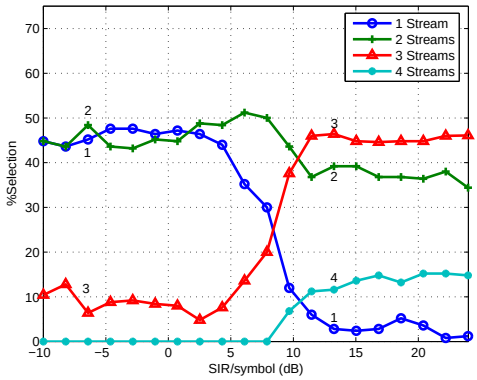

(a) OL-SDMA, stream control with deterministic antenna selection.

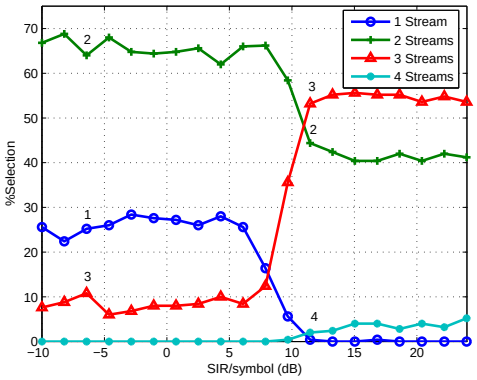

(b) OL-SDMA, stream control with optimal antenna selection.

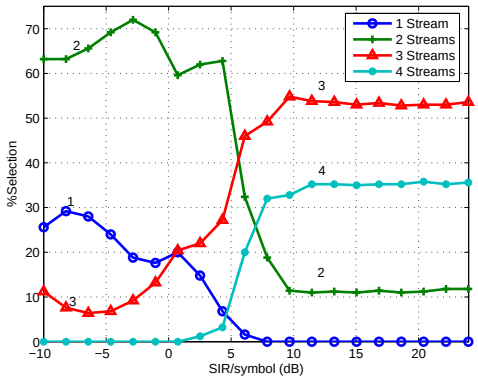

(c) CL-SDMA, stream control using whitened channel information.

Figure 14: Number of streams used by one link with different MIMO configurations for different SIR values. Target BER = 10^{-5}

interference is strong, SIR $<$ 9dB, the link mostly uses one or two streams with about equal probability. This leads to receive diversity gain, which is critical in satisfying the target BER. The use of optimal antenna selection along with stream control results in higher selection probability for two streams compared to one stream. This is because with optimal antenna selection, transmit diversity gain is also available and as the link can afford two streams more often. Thus optimal antenna selection-aided stream control enables OL-SDMA to exploit spatial multiplexing better than

the deterministic selection.

From 14(b), we also note that at high SIR, OL-SDMA with optimal selection-aided stream control rarely chooses 4 streams, thus resulting in lower throughput compared to CL-SDMA with stream control, as shown in 12. Finally, Figure 14(c) shows the optimal stream control that could be achieved by CL-SDMA using whitened channel information. We observe that unlike OL-SDMA, both with and without optimal antenna selection, CL-SDMA rarely uses one or two streams when interference is relatively weak. It is important to note that the link throughput is dependent not only on the number of streams used, but also on the number of bits carried by each stream.

4.3 Summary

In this chapter, we have analyzed the performance gains offered by the use of stream control for interfering MIMO links with linear MMSE receiver processing. Although, CL-SDMA with stream control using whitened channel information offers the best throughput, it has substantial overhead of providing the CSI to all the transmit nodes. However, the use of optimal transmit antenna selection in conjunction with stream control algorithm for OL-MIMO is an attractive alternative to CL-MIMO as it incurs a minimal overhead of specifying the chosen antenna set.

CHAPTER V

MSE OPTIMAL ANTENNA SELECTION

In Chapters 3 and 4, we demonstrated the importance of optimal antenna selection in conjunction with stream control for improving the performance of OL-SDMA networks. Though, one major challenge in employing stream control with optimal selection is the search of optimal subset of antennas. This chapter presents an optimal MSE-based selection framework for developing computationally efficient antenna selection algorithms that work particularly well in terms of the BER of SM-MIMO receivers that use linear processing.

Antenna subset selection problems involve the choice of appropriate cost function (e.g., capacity, bit error rate) and a methodology to determine the antenna subset that optimizes the cost function. One of the most straightforward selection approach is to evaluate the cost function over all possible antenna subsets. However, it quickly becomes computationally prohibitive with increasing number of combinations. Various suboptimal antenna selection schemes for SM-MIMO systems have been studied in the recent literature [36, 22, 19, 43, 44, 35, 24, 23, 20, 27, 40]. A suboptimal algorithm that does not need to perform an exhaustive search over all possible subsets is proposed in [36]. Another promising approach for fast antenna selection was proposed by Gorokhov [22], and was later improved in [19]. In addition to these schemes, the norm-based selection (NBS) method is another popular algorithm [43, 19]. The NBS method selects the receive antennas corresponding to the rows of the channel matrix with the largest Euclidean norms. Indeed, the main drawback of the NBS is that it may lead to much lower capacity in the presence of receive correlation [19]. Most of these studies assume channel capacity as the cost function instead of the more practical bit error rate (BER) metric, which is dependent on the receiver processing.

Since the receivers with practical complexity cannot achieve the channel capacity, the antenna selection methods based on the capacity optimization are bound to be inefficient with respect to the error performance of these receivers.

Antenna selection algorithms to minimize the BER in linear receivers has been addressed recently [21, 4, 3, 25, 33, 54]. A transmit antenna selection mechanism for ZF receivers is proposed in [21] to mitigate the effect of transmit antenna correlation. The proposed selection algorithm uses the transmit correlation matrix to determine the antenna subset. Since the proposed algorithm does not exploit the information based on instantaneous channel matrix, it cannot achieve full transmit diversity. In [4] Berenguer et al. proposed a transmit antenna selection algorithm based on the geometrical interpretation of the decoding process for ZF receivers. This work was later extended to lattice-reduction-aided (LRA) ZF receivers in [3]. The authors also proposed an approximate selection rule for LRA MMSE receivers based on the minimization of maximum MSE [3, Eq (24)]. A multimode antenna selection approach for improving the error performance of SM-MIMO is reported in [25]. The proposed scheme dynamically controls both the number of substreams transmitted and the mapping of substreams to a subset of transmit antennas, resulting in additional array gain.

In the following sections, we first outline the system model for developing antenna selection framework in the following section. Next, we develop sub-optimal transmit/receive antenna selection algorithms and present simulation results considering both isolated and interference-limited channels. These algorithms are greedy in nature and attempt to minimize the MSE at each step when an antenna is added (or removed) from the selected subset.

5.1 System Model

We consider a spatial multiplexing system with N_t transmit antennas and N_r receive antennas .The channel is flat-fading and slowly time varying. It is unknown at the transmitter but is known at the receiver. A low bandwidth, zero-delay, error-free feedback link provides limited channel information from the receiver to the transmitter.

During each symbol time, L_t input symbols are multiplexed for transmission over L_t transmit antennas. The subset of transmit antennas is determined by a selection algorithm operating at the receiver. Via the feedback path, the receiver sends the transmitter the optimal subset $S \in \mathbf{S}$, where $\mathbf{S}$ is the set of all possible $\binom{N_t}{L_t}$ subsets of transmit antennas.

Let $\mathbf{H}_{N_t \times N_t}$ denote the $N_r \times N_t$ channel matrix and let $\mathbf{H}_S$ denote the $N_r \times L_t$ submatrix corresponding to transmit antenna subset S. The corresponding vector of received complex baseband samples after matched filtering is given by

$$\mathbf{r} = \mathbf{H}_S \mathbf{a} + \mathbf{n}, \tag{28}$$

where $\mathbf{a}$ denotes the transmitted vector and $\mathbf{n}$ is the additive white noise. The noise components are assumed to be uncorrelated with complex variance σ_n^2. The inputs are chosen from same unit-energy constellation and are uncorrelated so that $\mathrm{E}[\mathbf{a}\mathbf{a}^H] = \mathbf{I}$, where E[.] denotes the expected value of its argument.

5.2 Antenna Selection Methodology

Let the receiver employ a linear detector, C, so that the mean-square error (mse) is given by

$$\begin{aligned} mse &= E[||\mathbf{C}\mathbf{r} - \mathbf{a}||^2] \\ &= \mathrm{tr}\Big(\underbrace{E[(\mathbf{C}\mathbf{r} - \mathbf{a})(\mathbf{C}\mathbf{r} - \mathbf{a})^H]}_{\mathbf{W}} \Big), \end{aligned} \tag{29}$$

where ||.|| denotes the Euclidean norm of the vector argument and tr(.) denotes the trace of its argument. Now the matrix $\mathbf{W}$ in (29) can also be written as [2]

$$\mathbf{W} = (\mathbf{C} - \mathbf{H}_S^H \mathbf{R}^{-1})\mathbf{R}^{-1}(\mathbf{C} - \mathbf{H}_S^H \mathbf{R}^{-1})^H + \mathbf{I} - \mathbf{H}_S^H \mathbf{R}^{-1}\mathbf{H}, \tag{30}$$

where $\mathbf{R} = N_o\mathbf{I} + \mathbf{H}_S\mathbf{H}_S^H$. Since only the first term in (30) depends on $\mathbf{C}$, MMSE solution chooses $\mathbf{C} = \mathbf{H}_S^H\mathbf{R}^{-1}$ to make it zero. The term $\mathrm{tr}(\mathbf{I} - \mathbf{H}_S^H\mathbf{R}^{-1}\mathbf{H}_S)$ represents the *mse*. Optimal antenna selection must choose the transmit antennas so as to minimize the *mse*. Observing that *mse* is minimized when $\mathrm{tr}(\mathbf{H}_S^H\mathbf{R}^{-1}\mathbf{H}_S)$ is maximized and using the trace identity $\mathrm{tr}(\mathbf{XY}) = \mathrm{tr}(\mathbf{YX})$, optimal antenna selection solution can be obtained as

$$\mathbf{S}_{mmse} = \underset{\mathbf{H}_S \in \mathbf{H}_{N_t}}{\arg\max}\, \mathrm{tr}(\mathbf{H}_S\mathbf{H}_S^H\mathbf{R}^{-1}), \tag{31}$$

where $\mathbf{S}_{mmse}$ denotes the subset of selected antennas and $\mathbf{H}_{N_t}$ denotes the $N_r \times N_r$ channel matrix. To select the antennas in the optimal way, the trace involving matrix inversion has to be computed for $\binom{N_t}{L_t}$ possible combinations. This could be computationally burdensome when the number of antenna combinations is large. In the following section, we present several reduced complexity antenna selection algorithms. Looking at (31), we observe that as $N_o \to 0$, $\mathbf{C} \to \mathbf{H}_S^H(\mathbf{H}_S\mathbf{H}_S^H)^{-1}$, which is the Zero-Forcing (ZF) filter. Therefore, all the algorithms presented in this chapter for MMSE receiver can also be applied to ZF receiver by choosing a sufficiently small value for N_o.

5.3 Transmit Antenna Selection

As described in the previous section, (31) can be used to determine the optimal subset of transmit antennas. However, (31) involves matrix inversion and large number of choices will make the search prohibitive. In the following subsections, we present two greedy solutions that are suboptimal but efficient. Both greedy algorithms try to

maximize the trace in (31) at each intermediate step. An antenna is selected/removed so that doing so leads to maximum increase in trace.

5.3.1 No Interference

5.3.1.1 Incremental Transmit Antenna Selection (ITAS)

The algorithm begins with an empty set of selected antennas and selects one antenna in each step. After n steps, there are n selected antennas and the corresponding channel matrix is denoted by $\mathbf{H}_n$. The matrix $\mathbf{H}_n$ consists of the columns of $\mathbf{H}_{N_t}$ in the same order as they appear in $\mathbf{H}_{N_t}$. We will denote the k^{th} column of by $\mathbf{h}_k$ and will use the following notations

$$\mathbf{B}_n = \left(\mathbf{I} + \frac{1}{N_o}\mathbf{H}_n\mathbf{H}_n^H\right)^{-1} \tag{32}$$

$$\Delta_n = \mathrm{tr}(\mathbf{H}_n\mathbf{H}_n^H\mathbf{B}_n), \tag{33}$$

where the subscript n denotes the n^{th} step. Now if in the $(n+1)^{st}$ step, transmit antenna corresponding to the k^{th} column of $\mathbf{H}_{N_t}$ is selected, then $\mathbf{h}_k$ is inserted in proper position in $\mathbf{H}_n$ to obtain the channel matrix $\mathbf{H}_{n+1}$. The matrices in (33) are updated as

$$\mathbf{H}_{n+1}\mathbf{H}_{n+1}^H = \mathbf{H}_n\mathbf{H}_n^H + \mathbf{h}_k\mathbf{h}_k^H \tag{34}$$

$$\mathbf{B}_{n+1} = \mathbf{B}_n - \frac{1}{N_o + \mathbf{h}_k^H\mathbf{B}_n\mathbf{h}_k}\mathbf{B}_n\mathbf{h}_k\mathbf{h}_k^H\mathbf{B}_n, \tag{35}$$

where (35) follows as a direct consequence of the matrix inversion lemma [34, (3.5.2.2)]. Using (34) and (35), the updated trace can be computed as

$$\begin{aligned}\Delta_{n+1} = \Delta_n &+ \mathrm{tr}[\mathbf{h}_k\mathbf{h}_k^H\mathbf{B}_n] \\ &- \frac{\mathrm{tr}[\mathbf{H}_n\mathbf{H}_n^H\mathbf{B}_n\mathbf{h}_k\mathbf{h}_k^H\mathbf{B}_n] + \mathrm{tr}[\mathbf{h}_k\mathbf{h}_k^H\mathbf{B}_n\mathbf{h}_k\mathbf{h}_k^H\mathbf{B}_n]}{N_o + \mathbf{h}_k^H\mathbf{B}_n\mathbf{h}_k}.\end{aligned} \tag{36}$$

Since $\mathbf{B}_n$ is a Hermitian matrix, we can use the identity $\text{tr}(\mathbf{XY}) = \text{tr}(\mathbf{XY})$ to further simplify (36) as

$$\begin{aligned} \text{tr}[\mathbf{h}_k\mathbf{h}_k^H\mathbf{B}_n] &= \mathbf{h}_k^H\mathbf{B}_n\mathbf{h}_k \\ \text{tr}[\mathbf{H}_n\mathbf{H}_n^H\mathbf{B}_n\mathbf{h}_k\mathbf{h}_k^H\mathbf{B}_n] &= ||\mathbf{h}_k^H\mathbf{B}_n\mathbf{H}_n||^2 \\ \text{tr}[\mathbf{h}_k\mathbf{h}_k^H\mathbf{B}_n\mathbf{h}_k\mathbf{h}_k^H\mathbf{B}_n] &= (\mathbf{h}_k^H\mathbf{B}_n\mathbf{h}_k)^2. \end{aligned} \tag{37}$$

Finally, substituting (37) in (36) and after some algebraic simplifications, we can express the change in the trace after the $(n+1)^{st}$ step as

$$\delta_{n+1,k} = \Delta_{n+1} - \Delta_n = \frac{N_o\mathbf{h}_k^H\boldsymbol{\beta}_{n,k} - ||\boldsymbol{\beta}_{n,k}^H\mathbf{H}_n||^2}{N_o + \mathbf{h}_k^H\boldsymbol{\beta}_{n,k}}, \tag{38}$$

where $\boldsymbol{\beta}_{n,k} = \mathbf{B}_n\mathbf{h}_k$, and $\delta_{n+1,k}$ represents the increase in the trace if k^{th} transmit antenna is selected in the $(n+1)^{st}$ step. Since our objective is to maximize the trace, we select the antenna whose contribution to the trace is the maximum. Thus the selection criteria is

$$P = \arg\max_k \delta_{n+1,k}. \tag{39}$$

To reduce the number of computations, $\boldsymbol{\beta}_{n+1,k}$ can be computed recursively as

$$\begin{aligned} \boldsymbol{\beta}_{n+1,k} &= \mathbf{R}_{n+1}\mathbf{h}_k \\ &= \mathbf{B}_n\mathbf{h}_k - \frac{\mathbf{B}_n\mathbf{h}_P\mathbf{h}_P^H\mathbf{B}_n\mathbf{h}_k}{N_o + \mathbf{h}_P^H\mathbf{B}_n\mathbf{h}_P} \\ &= \boldsymbol{\beta}_{n,k} - \boldsymbol{\beta}_{n,P}\frac{\mathbf{h}_P^H\boldsymbol{\beta}_{n,k}}{N_o + \mathbf{h}_P^H\boldsymbol{\beta}_{n,P}} \end{aligned} \tag{40}$$

assuming that $\mathbf{h}_P$ is selected in the n^{th} step. The proposed algorithm is summarized in Table 1 with the right column showing order of complexity of each step.

5.3.1.2 Decremental Transmit Antenna Selection (DTAS)

As the name suggests, the algorithm begins with full set of selected antennas and removes one antenna in each step. Thus at end of n^{th} step, n antennas are rejected

and $\mathbf{H}_{N_t-n}$ represents the channel matrix corresponding to remaining N_t-n antennas. The matrix $\mathbf{B}_n$ is defined as

$$\mathbf{B}_n = \left(\mathbf{I} + \frac{1}{N_o}\mathbf{H}_{N_t-n}\mathbf{H}_{N_t-n}^H\right)^{-1}. \tag{41}$$

If in the $(n+1)^{st}$ step, transmit antenna corresponding to k^{th} column of $\mathbf{H}_{N_t}$ is removed, then $\mathbf{R}_{n+1}$ is given by

$$\mathbf{B}_{n+1} = \mathbf{B}_n + \frac{1}{N_o - \mathbf{h}_k^H\mathbf{B}_n\mathbf{h}_k}\mathbf{B}_n\mathbf{h}_k\mathbf{h}_k^H\mathbf{B}_n, \tag{42}$$

where (42) is obtained using matrix inversion lemma [34, (3.5.2.2)]. Following the development similar to (34)-(38), the change in trace can be expressed as

$$\delta_{n+1,k} = \Delta_{n+1} - \Delta_n = \frac{||\boldsymbol{\beta}_{n,k}^H\mathbf{H}_n||^2 - N_o\mathbf{h}_k^H\boldsymbol{\beta}_{n,k}}{N_o - \mathbf{h}_k^H\boldsymbol{\beta}_{n,k}}, \tag{43}$$

where $\boldsymbol{\beta}_{n,k}$ is defined as in (38). Now the elimination criteria is to remove antenna whose removal leads to the maximum increase in trace, i.e,

$$P = \arg\max_k \delta_{n+1,k}. \tag{44}$$

It is not difficult to show that the vectors $\boldsymbol{\beta}_{n+1,k}$ can be updated as

$$\boldsymbol{\beta}_{n+1,k} = \boldsymbol{\beta}_{n,k} + \boldsymbol{\beta}_{n,P}\frac{\mathbf{h}_P^H\boldsymbol{\beta}_{n,k}}{N_o - \mathbf{h}_P^H\boldsymbol{\beta}_{n,P}}. \tag{45}$$

The algorithm along with the complexity analysis is outlined in Table 2. Let us compare the complexity of the two algorithms. For the single user case, ITAS doesn't require matrix inversion and has the lower complexity of $\mathrm{O}\big(\max(N_r, L_t^2)N_rN_t\big)$ compared to $\mathrm{O}(N_rN_t^2L_t)$ of transmit selection algorithm for LRA-ZF in [4, Table.1]. On the other hand, DTAS requires matrix inversion and has a complexity order of $\mathrm{O}\big(\max(N_t^3, N_r^2)N_r\big)$. Thus the ITAS algorithm has significantly lower complexity compared to the DTAS algorithm.

When only one antenna is selected, ITAS always finds the optimal solution as it requires just one step. Whereas when $N_t - 1$ transmit antennas are selected, DTAS

Algorithm 1 ITAS Algorithm

Require: $N_t, N_r, L_t, \sigma_n^2, \mathbf{H}_{N_t}$

Ensure: $N_r \geq N_t \geq L_t$	**Complexity**
$S := \{1, 2, ..., N_t\}$, $\mathbf{H} := [\ ]_{0\times 0}$	
$\mathbf{B} := \mathbf{I}$	
for $\forall k \in S$ **do**	
$\boldsymbol{\beta}_k := \mathbf{B}\mathbf{h}_k$	
end for	
for $n = 1$ to L_t **do**	
for $\forall k \in S$ **do**	
$\delta_k := \frac{N_o \mathbf{h}_k^H \boldsymbol{\beta}_k - \|\|\boldsymbol{\beta}_k^H \mathbf{H}\|\|^2}{N_o + \mathbf{h}_k^H \boldsymbol{\beta}_k}$	$\mathrm{O}(N_r N_t L_t^2)$
end for	
$P := \arg\max_k \delta_k$	$\mathrm{O}(N_t L_t)$
$S := S - \{P\}$	
$\mathbf{H} := [\mathbf{H}, \mathbf{h}_p]$	
for $\forall k \in S$ **do**	
$\boldsymbol{\beta}_k := \boldsymbol{\beta}_k - \boldsymbol{\beta}_P \frac{\mathbf{h}_P^H \boldsymbol{\beta}_k}{N_o + \mathbf{h}_P^H \boldsymbol{\beta}_P}$	$\mathrm{O}(N_r N_t L_t)$
end for	
end for	
return $\{1, 2, ...N_t\} - S$	

yields the optimal solution. It is intuitive to think that if ITAS takes fewer steps compared to DTAS, then it is more likely to yield optimal solution than the DTAS algorithm and vice versa.

5.3.2 Co-channel Interference

Let us consider a system where cochannel interference is present from K other users. Let $\mathbf{G}_i$ denote the normalized channel matrix between the i^{th} interferer and the desired receiver. Now, the vector of received complex baseband samples after matched filtering can be expressed as

$$\mathbf{r} = \mathbf{H}\mathbf{a} + \sum_{i=1}^{K} \mathbf{G}_i \mathbf{x}_i^H + \mathbf{n}, \tag{46}$$

where $\mathbf{x}_i$ represents the normalized transmitted signal from the i^{th} interferer. The noise vector and the channel matrices $\mathbf{G}_i$ have independent and identically distributed zero means and unit variance complex Gaussian entries. For simplicity, we assume

Algorithm 2 DTAS Algorithm

Require: $N_t, N_r, L_t, N_o, \mathbf{H}_{N_t}$

Ensure: $N_r \geq N_t \geq L_t$	**Complexity**
1: $S := \{1, 2, ..., N_t\}$, $\mathbf{H} := \mathbf{H}_{N_t}$	
2: $\mathbf{B} := \left(\mathbf{I}_{N_r} + \frac{1}{N_o}\mathbf{H}_{N_t}\mathbf{H}_{N_t}^H\right)^{-1}$	$\mathrm{O}(N_r^3)$
3: **for** $\forall k \in S$ **do**	
4: $\quad \boldsymbol{\beta}_k := \mathbf{B}\mathbf{h}_k$	$\mathrm{O}(N_r^2 N_t)$
5: **end for**	
6: **for** $n = 1$ to $N_t - L_t$ **do**	
7: $\quad$ **for** $\forall k \in S$ **do**	
8: $\quad\quad \delta_k := \frac{\|\boldsymbol{\beta}_k^H \mathbf{H}\|^2 - N_o \mathbf{h}_k^H \boldsymbol{\beta}_k}{N_o - \mathbf{h}_k^H \boldsymbol{\beta}_k}$	$\mathrm{O}(N_r N_t^3)$
9: $\quad$ **end for**	
10: $\quad P := \arg\max_k \delta_k$	$\mathrm{O}(N_t^2)$
11: $\quad S := S - \{P\}$	
12: $\quad \mathbf{H} := \mathbf{H} - \{\mathbf{h}_p\}$	
13: $\quad$ **for** $\forall k \in S$ **do**	
14: $\quad\quad \boldsymbol{\beta}_k := \boldsymbol{\beta}_k + \boldsymbol{\beta}_P \frac{\mathbf{h}_P^H \boldsymbol{\beta}_k}{N_o - \mathbf{h}_P^H \boldsymbol{\beta}_P}$	$\mathrm{O}(N_r N_t^2)$
15: $\quad$ **end for**	
16: **end for**	
return S	

all of the interfering signals $\mathbf{x}_i$, $\forall i \in (1, K)$, are unknown to the receiver. This model is well suited to the case where each user chooses his signaling without knowing the exact interference environment he will face. If we assume that the power covariance matrix of $\mathbf{x}_i$ is $\mathrm{E}[\mathbf{x}_i \mathbf{x}_i^H] = \mathbf{I}$, then the covariance matrix of received vector $\mathbf{r}$ can be obtained as

$$\mathbf{R} = \mathrm{E}[\mathbf{r}\mathbf{r}^H] = \mathbf{H}\mathbf{H}^H + \sum_{i=1}^{K} \mathbf{G}_i \mathbf{G}_i^H + N_o \mathbf{I}. \tag{47}$$

Now, the matrix $\mathbf{B}$ used in Table 1 and Table 2 can be obtained as

$$\mathbf{B} = \begin{cases} N_o\left(\mathbf{R} - \mathbf{H}\mathbf{H}^H\right)^{-1} & for \text{ ITAS} \\ N_o \mathbf{R}^{-1} & for \text{ DTAS} \end{cases} \tag{48}$$

It is apparent that in presence of cochannel interference, the computational complexity associated with the Steps 2 and 4 of the ITAS algorithm becomes the same as in the DTAS algorithm, thus removing any computational advantage offered by the

former.

5.4 Receive Antenna Selection

For spatial multiplexing systems, receive antenna selection is an effective, low-complexity means to provide diversity gain to the data streams. Antenna selection at the receiver plays an even more important role in interference-limited channels. In the following subsections, we present greedy solutions for receive antenna selection.

5.4.1 No Interference

5.4.1.1 Incremental Receive Antenna Selection (IRAS)

The algorithm works in a similar fashion as the incremental transmit antenna selection algorithm presented in the previous section. In each step, we select the row vector that leads to minimal increase in the trace given by (31). Let us use the following notations

$$\mathbf{B}_n = \left(\mathbf{I} + \frac{1}{N_o}\mathbf{H}_n^H\mathbf{H}_n\right)^{-1} \tag{49}$$

$$\Delta_n = \mathrm{tr}(\mathbf{B}_n), \tag{50}$$

where $\mathbf{B}_0 = \mathbf{I}$ is the initial condition for the algorithm. Now if in the $(n+1)^{st}$ step, the k^{th} row of $\mathbf{H}$, $\mathbf{r}_k$, is selected then $\mathbf{B}_{n+1}$ can be updated using matrix inversion lemma [34, (3.5.2.2)] as

$$\mathbf{B}_{n+1} = \mathbf{B}_n - \frac{1}{N_o + \mathbf{r}_k\mathbf{B}_n\mathbf{r}_k^H}\mathbf{B}_n\mathbf{r}_k^H\mathbf{r}_k\mathbf{B}_n. \tag{51}$$

Thus the change in trace after the $(n+1)^{st}$ step can be easily computed as

$$\delta_{n+1,k} = \Delta_{n+1} - \Delta_n = \frac{-||\boldsymbol{\alpha}_{n,k}||^2}{N_o + \boldsymbol{\alpha}_{n,k}\mathbf{r}_k^H}, \tag{52}$$

where $\boldsymbol{\alpha}_{n,k} = \mathbf{r}_k\mathbf{B}_n$. The selection rule is to choose the antenna that leads to minimum increase in trace, i.e,

$$P = \arg\min_k \delta_{n+1,k}. \tag{53}$$

Algorithm 3 IRAS Algorithm

Require: $N_t, N_r, L_r, N_o, \mathbf{H}_{N_r}$

Ensure: $N_r \geq L_r \geq N_t$ **Complexity**

$S := \{1, 2, ..., N_r\}$

$\mathbf{B} := \mathbf{I}_{N_t}$

for $\forall k \in S$ **do**

  $\boldsymbol{\alpha}_k := \mathbf{r}_k \mathbf{B}$

end for

for $n = 1$ to L_r **do**

  for $\forall k \in S$ **do**

    $\delta_k := \frac{-||\boldsymbol{\alpha}_k||^2}{N_o + \boldsymbol{\alpha}_k \mathbf{r}_k^H} \mathbf{r}_k^H$ $\mathrm{O}(N_r N_t L_r)$

  end for

  $P := \arg\min_k \delta_k$ $\mathrm{O}(N_r L_r)$

  $S := S - \{P\}$

  for $\forall k \in S$ **do**

    $\boldsymbol{\alpha}_k := \boldsymbol{\alpha}_k - \boldsymbol{\alpha}_P \frac{\boldsymbol{\alpha}_k \mathbf{r}_P^H}{N_o + \boldsymbol{\alpha}_P \mathbf{r}_P^H}$ $\mathrm{O}(N_r N_t L_r)$

  end for

end for

return $\{1, 2, ...N_r\} - S$

The vectors $\boldsymbol{\alpha}_{n+1,k}$ can be recursively computed as

$$\boldsymbol{\alpha}_{n+1,k} = \boldsymbol{\alpha}_{n,k} - \boldsymbol{\alpha}_{n,P} \frac{\boldsymbol{\alpha}_{n,k} \mathbf{r}_P^H}{N_o + \boldsymbol{\alpha}_{n,P} \mathbf{r}_P^H}. \tag{54}$$

The algorithm is summarized in Table 3 with the right column showing the complexity corresponding to each part of the algorithm.

5.4.1.2 Decremental Receive Antenna Selection (DRAS)

The algorithm is quite similar to the DTAS algorithm presented in the previous section. For the sake of brevity we omit the development and present the implementation in Table 4. From Tables 3 and 4, it is apparent that IRAS has significantly lower complexity, $\mathrm{O}(N_t N_r L_r)$, compared to $\mathrm{O}\big(\max(N_t^2, N_t N_r, N_r^2) N_t\big)$, that of the DRAS algorithm. Observing that $N_t \leq N_r$ is always satisfied to avoid overloading the receiver, complexity order of DRAS algorithm can be expressed as $\mathrm{O}(N_t N_r^2)$. The performance relationship between the two algorithms is same as between ITAS and DTAS algorithms.

Algorithm 4 DRAS Algorithm

Require: $N_t, N_r, L_r, N_o, \mathbf{H}_{N_r}$

Ensure: $N_r \geq L_r \geq N_t$	**Complexity**
$S := \{1, 2, ..., N_r\}$	
$\mathbf{B} := \left(\mathbf{I}_{N_t} + \frac{1}{N_o}\mathbf{H}_{N_r}^H \mathbf{H}_{N_r}\right)^{-1}$	$\mathrm{O}(N_t^3)$
for $\forall k \in S$ **do**	
$\quad \boldsymbol{\alpha}_k := \mathbf{r}_k \mathbf{B}$	$\mathrm{O}(N_r N_t^2)$
end for	
for $n = 1$ to $N_r - L_r$ **do**	
$\quad$ **for** $\forall k \in S$ **do**	
$\quad\quad \delta_k := \frac{\|\|\boldsymbol{\alpha}_k\|\|^2}{N_o - \boldsymbol{\alpha}_k \mathbf{r}_k^H} \mathbf{r}_k^H$	$\mathrm{O}(N_r^2 N_t)$
$\quad$ **end for**	
$\quad P := \arg\min_k \delta_k$	$\mathrm{O}(N_r^2)$
$\quad S := S - \{P\}$	
$\quad$ **for** $\forall k \in S$ **do**	
$\quad\quad \boldsymbol{\alpha}_k := \boldsymbol{\alpha}_k + \boldsymbol{\alpha}_P \frac{\boldsymbol{\alpha}_k \mathbf{r}_P^H}{N_o - \boldsymbol{\alpha}_P \mathbf{r}_P^H}$	$\mathrm{O}(N_r^2 N_t)$
$\quad$ **end for**	
end for	
return S	

5.4.2 Co-channel Interference

Unlike transmit antenna selection, it is difficult to obtain optimal solution for receive antenna selection using the receive covariance matrix, $\mathbf{R}$. However, an approximate solution can be obtained using the simple channel whitening approach of [5] as

$$\widetilde{\mathbf{H}} = \mathbf{T}^{-1/2}\mathbf{H}, \tag{55}$$

where $\mathbf{T}$ represents the noise plus interference covariance matrix. It is interesting to note that such an approach leads to fairly good antenna selection as will be shown below.

5.5 Simulation Results

In this section we present the simulation results on the BER performance of the proposed antenna selection algorithms and compare them against some of the existing

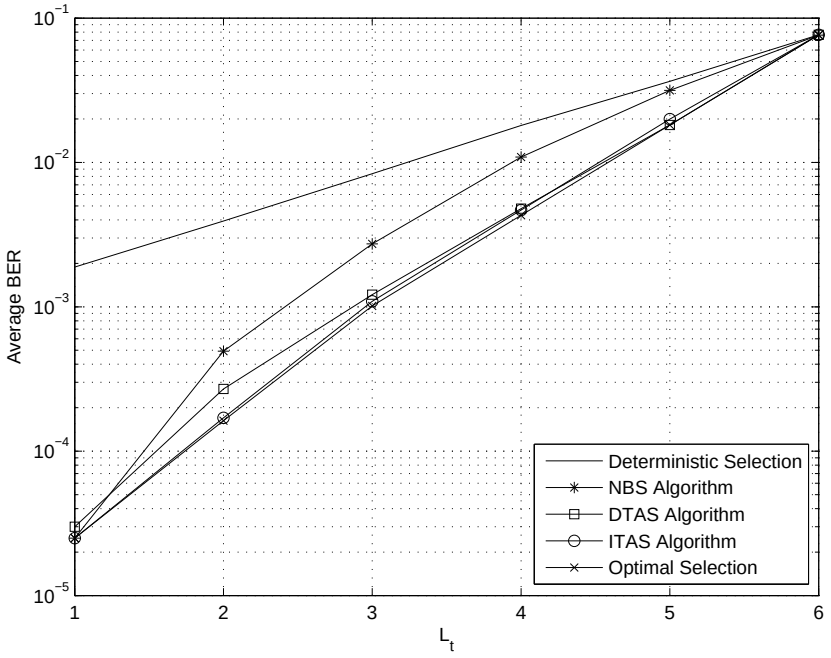

Figure 15: MMSE error performance for (6,6) MIMO system with varying number active transmit antennas and $SNR = 5dB$.

antenna selection techniques [24, 23, 20, 21, 4]. For the sake of completeness, in all the figures, we also show the performance curves corresponding to deterministic and NBS selection. All simulation results assume an independent and identically distributed (i.i.d) Rayleigh fading channel unless specified otherwise. Simulations results are generated using Monte Carlo simulation of 10^6 channel realizations. Throughout our simulations, we assume 16-QAM modulation.

In the first example, we consider an isolated MIMO link with linear MMSE receiver. Figure 15 shows the BER performance versus L_t for SNR = 5 dB. It is apparent that all antenna selection algorithms perform significantly better than the deterministic selection, which can't exploit transmit diversity. In particular, the proposed ITAS and DTAS algorithms offer close to optimal performance. The ITAS and NBS algorithms are both optimal for $L_t = 1$. Whereas, for $L_t = N_t - 1$, DTAS algorithm yields optimal performance. As a general rule of thumb, ITAS algorithm

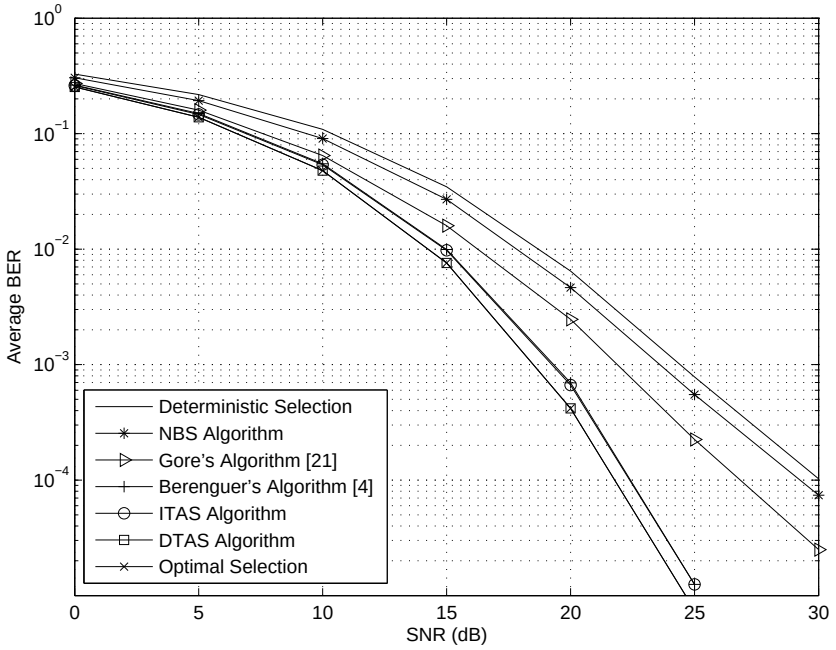

Figure 16: Error performance of (4,4) MIMO system with ZF receiver in the presence of transmit correlation. Three transmit antennas are selected.

is preferable when $L_t < N_t/2$ whereas for $L_t > N_t/2$, DTAS is desirable.

From Figure 15, it is also interesting to note that as number of selected antennas increases, the BER performance of deterministic selection deteriorates less rapidly compared to other antenna selection algorithms. This can attributed to the fact that the diversity gain associated with the deterministic selection comes only from the receive diversity, which reduces as more streams are added. Contrary to this, the proposed transmit antenna selection algorithms help achieve transmit diversity gain resulting in an overall diversity gain of $(N_t - L_t)(N_r - L_t)$, which decreases more rapidly with increasing L_t.

Next, we consider a (4,4) MIMO link with ZF receiver and assume transmit correlation but no correlation at the receiver. Figure 16 compares the BER performance of the proposed algorithms against Gore's Algorithm [21] and Berenguer's algorithm [4]. The transmit correlation matrix, $\mathbf{R_t}$, used in the simulations is same as in [21,

Eq. (15)]. Gore's algorithm uses the transmit correlation information to select antennas that minimize the error probability of the worst stream. The selected antennas are $\{1, 2, 4\}$ for the transmit correlation matrix, $\mathbf{R_t}$. It, obviously, is not an optimal strategy because all the streams and not just the worst stream determine the error performance of a linear receiver.

From Figure 16, we observe that although Gore's algorithm performs almost 3 dB better than non-optimal deterministic selection, which selects $\{1, 2, 3\}$, it fails to exploit the full transmit diversity that can be achieved by choosing optimal set of transmit antennas for each channel realization. For example, when the channel is in deep fade, it is better to choose two strongly correlated but un-faded streams and an uncorrelated stream in deep fade rather than all three uncorrelated streams with two being in deep fade. It can also be noted that Berenguer's transmit antenna selection algorithm for ZF receiver performs very close to the ITAS algorithm but is still 1 dB worse than the DTAS algorithm, which is optimal in this case.

Figure 17 shows the BER performance of various sub-optimal selection approaches in the presence of fixed co-channel interference assuming i.i.d Rayleigh faded channels. The interference is assumed to be resulting from another MIMO transmitter using 3 antennas. The desired transmitter is equipped with 6 antennas and chooses 3 antennas to improve the BER performance of the desired link. From Figure 17, it is apparent that the BER curves for both deterministic selection and NBS selection are relatively flat. This is because the receiver, in the absence of transmit diversity, uses additional 3 antennas to suppress the interference and thus no diversity gain is rendered to the desired streams. On the other hand, the proposed algorithms, ITAS and DTAS, are able to exploit transmit diversity better and provide reasonably good BER performance. The robustness of the proposed algorithms is further highlighted when the interference power increases to 0 dB, which causes only a minimal degradation in the BER performance.

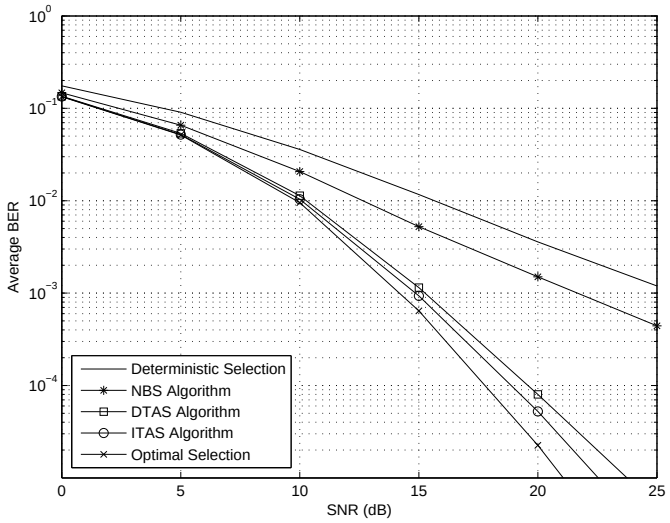

(a) SIR = 10 dB

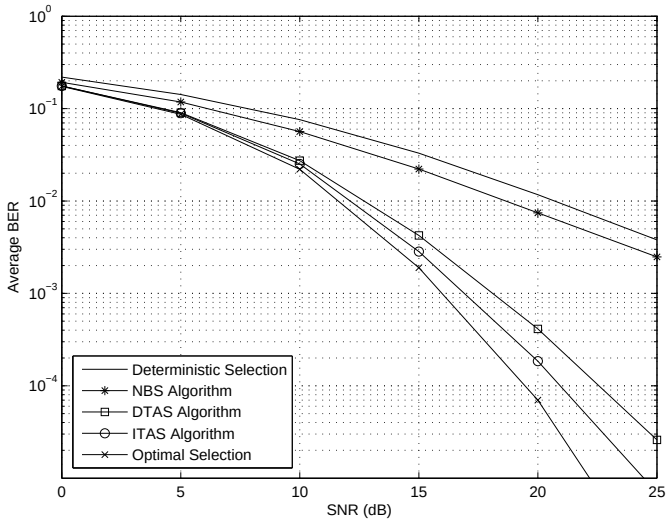

(b) SIR = 0 dB

Figure 17: MMSE error rate for (6,6) MIMO link in presence of co-channel interference from 3 other streams. Three transmit antennas are selected.

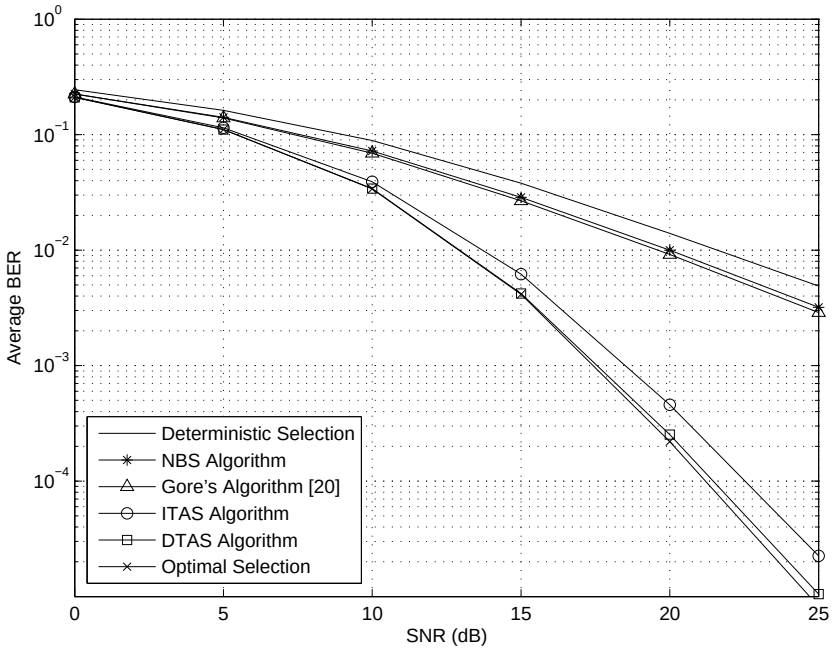

Figure 18: MMSE error rate for (6,4) MIMO system. Four receive antennas are selected.

Figure 18 illustrates the error performance of various receive antenna selection algorithms for the MMSE receiver. We notice that Gore's algorithm [20], which chooses antennas that maximize the capacity, is only slightly better than the NBS algorithm and performs much worse than the optimal solution. It is evident that sub-optimal receive algorithms yield near-optimal performances. In particular, DRAS algorithm performs better than the ITAS algorithm as it requires 2 iterations compared to 4 for the latter.

Figure 19 shows the BER performance of different receive antenna selection algorithms in the presence of fixed co-channel interference. The (6,2) MIMO system is subjected to co-channel interference from 2 other streams with equal power as the desired streams. The selections algorithms choose 4 receive antennas that minimize the link error. It is evident that optimal selection approach, which assumes interferer's channel knowledge, performs the best. Whereas the IRAS and DRAS algorithms, in

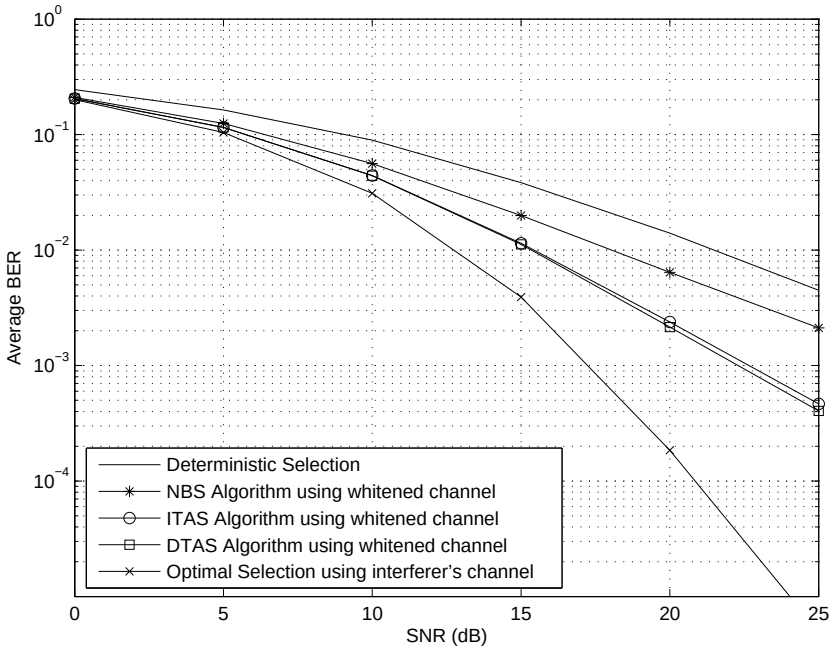

Figure 19: BER performance of MMSE receiver for (6,2) MIMO system in the presence of 2 interfering streams with SIR = 0dB. Four receive antennas are selected.

the absence of interferer's channel knowledge, provide significant improvement over deterministic and NBS selection. It was also found that as the SIR is increased, the gap between the proposed algorithms and the optimal selection approach is considerably reduced.

5.6 Summary

In this chapter, we have presented new computationally efficient algorithms for transmit and receive antenna selection for linear receivers. The presented algorithms are also applicable to handle fixed co-channel interference and offer near optimal BER performance both in presence of transmit correlation and co-channel interference. In absence of co-channel interference, incremental selection algorithms have much lower complexity compared to the decremental selectional algorithms and are therefore more attractive.

CHAPTER VI

MULTIUSER DETECTION FOR STBC USERS

In the previous chapters we considered closed-loop or transmitter selection Spatial Multiplexing (SM) MIMO systems, which offer extremely high spectral efficiencies. These systems require explicit feedback paths for communicating full or partial CSI to the transmitter for computing the power allocation matrices. However, the transmission errors in the feedback channel may adversely affect the performance of such systems. Also, the bandwidth requirements for the feedback channel along with errors in the feedback path may altogether reduce the effective throughput gains offered by SM-MIMO systems.

In this chapter, we focus our attention to Space-Time Block Codes (STBCs), which offer transmit diversity gains without requiring any explicit channel feedback [1, 48]. The temporal and spatial structure of certain STBCs, called orthogonal STBCs (OSTBCs), offer the additional advantage of maximum likelihood detection based only on linear processing at the receiver [48]. As a result, the OSTBCs, especially the Alamouti code [1], are being widely adopted in various wireless communication standards such as the 3GPP cellular standard, WiMAX (IEEE 802.16), and IEEE 802.11n. These standards do not allow co-channel interference among different users. However, in a multiuser environment, the network performance can be significantly improved if spatial diversity is exploited by allowing controlled co-channel transmissions [41]. In this chapter, we explore co-channel interference problem and propose IC techniques for OSTBCs with 3 and 4 antennas which can apply to an SDMA MAC.

Despite the low data rates supported by various STBCs, they are attractive from a network point of view as they cause correlated interference, which can be mitigated using only one additional antenna without sacrificing space-time diversity gains. In

[37], Naguib et al. developed a minimum mean square error (MMSE) interference suppression technique for two co-channel users employing the Alamouti code [1]. It was shown that the impact of co-channel interference can be completely eliminated by adding one more receive antenna without sacrificing space-time diversity gains. This scheme was later extended to frequency-selective channels in [53]. In [29] authors extend the work of [37] to the interference cancellation (IC) and detection for users with 4 transmit antennas using quasi-orthogonal space-time block coding [26]. In another related work, Stamoulis et al. [45] presented a simple suboptimal linear processing scheme that achieves IC of two co-channel users employing any rate-1/2 complex STBC based on an orthogonal design. Like [37], [45] cancels the correlated STBC interference with the aid of additional receive antenna while preserving the diversity gains. However, the method is based on 2-stage receive processing and is not optimal in terms of mean square error (MSE).

In contrast to [45], the algorithm presented in this chapter is single-stage and MMSE-optimal. In contrast to [37], the proposed algorithm treats unity rate real and derived rate-1/2 complex OSTBCs for 3 and 4 transmit antennas [48]. Like [37] and [45], the algorithm requires only one additional antenna to cancel an OSTBC interference. Some special algebraic properties of linear OSTBCs are exploited to make the algorithm have low complexity.

6.1 Real STBC and IC of Two Co-channel Users

In this section, we focus on the MMSE-based multiuser detection of two synchronous co-channel users, each employing the same real STBCs. We will show for $n_t = 3$ or 4, the linear receiver processing can be implemented without matrix inversions, and after the IC-stage, the symbols are recovered with space-time diversity gain.

Let us use subscripts 1 and 2 to differentiate between the corresponding channel matrices and symbol vectors of the two users. Thus the received baseband vector is

given by

$$\mathbf{y}' = \mathbf{F}'_{\mathbf{1}}\mathbf{s_1} + \mathbf{F}'_{\mathbf{2}}\mathbf{s_2} + \mathbf{v}' = \mathbf{F}'\mathbf{s} + \mathbf{v}' \tag{56}$$

where $\mathbf{F}_i$'s are defined as in (13), $\mathbf{F} = \begin{pmatrix} \mathbf{F}_1 & \mathbf{F}_2 \end{pmatrix}$, and $\mathbf{s} = \begin{pmatrix} \mathbf{s}_1^T & \mathbf{s}_2^T \end{pmatrix}^T$. Let us assume that the receiver employs the MMSE filter given by $\mathbf{C} = (\mathbf{F}'^T\mathbf{F}' + N_o\mathbf{I})^{-1}\mathbf{F}'^T$, where N_o denotes the noise variance. It is not difficult to see that $\mathbf{F}'^T\mathbf{F}' = \mathrm{Re}(\mathbf{F}^H\mathbf{F})$. Exploiting the channel decoupling property of orthogonal STBCs, $\mathrm{Re}(\mathbf{F}_i^H\mathbf{F}_i) = ||\mathbf{H}_i||^2\mathbf{I}$ [32, (7.4.1.4)], we can simplify $\mathbf{F}'^T\mathbf{F}'$ as

$$\mathbf{F}'^T\mathbf{F}' = \begin{pmatrix} ||\mathbf{H}_1||^2\mathbf{I} & \mathbf{R}_{12} \\ \mathbf{R}_{12}^T & ||\mathbf{H}_2||^2\mathbf{I} \end{pmatrix}, \tag{57}$$

where $\mathbf{R}_{12} = \mathrm{Re}(\mathbf{F}_1^H\mathbf{F}_2)$ and $||.||$ denotes the Frobenius norm of the matrix argument. Now the matrix inversion component of MMSE filter can be simplified using (57) with the aid of block matrix inversion [34, (3.5.3.1)], as

$$(\mathbf{F}'^T\mathbf{F}' + N_o\mathbf{I})^{-1} = \begin{pmatrix} (||\mathbf{H}_2||^2 + N_o)\mathbf{\Gamma} & -\mathbf{R}_{12}\mathbf{\Gamma} \\ -\mathbf{\Gamma}\mathbf{R}_{12}^T & (||\mathbf{H}_1||^2 + N_o)\mathbf{\Gamma} \end{pmatrix}, \tag{58}$$

where

$$\mathbf{\Gamma} = \Big((||\mathbf{H}_1||^2 + N_o)(||\mathbf{H}_2||^2 + N_o)\mathbf{I} - \mathbf{R}_{12}\mathbf{R}_{12}^T\Big)^{-1}. \tag{59}$$

Next, by multiplying both sides of (58) on the right by $(\mathbf{F}'^T\mathbf{F}' + N_o\mathbf{I})$, substituting $\mathbf{F}'^T\mathbf{F}'$ with (57), and equating the $(2,1)^{th}$ sub-matrix element of the resulting product to $\mathbf{0}$, we get $\mathbf{R}_{12}^T\mathbf{\Gamma} = \mathbf{\Gamma}\mathbf{R}_{12}^T$. Exploiting the self-adjoint nature of $\mathbf{\Gamma}$, it can be further shown $\mathbf{\Gamma}$ also commutes with $\mathbf{R}_{12}$, i.e.,

$$\mathbf{R}_{12}\mathbf{\Gamma} = \mathbf{\Gamma}\mathbf{R}_{12}. \tag{60}$$

Using (58)-(60), the resulting MMSE filter can be expressed in a particularly useful form as

$$\mathbf{C} = \begin{pmatrix} \mathrm{Re}(\mathbf{W}_{1,2}) & -\mathrm{Im}(\mathbf{W}_{1,2}) \\ \mathrm{Re}(\mathbf{W}_{2,1}) & -\mathrm{Im}(\mathbf{W}_{2,1}) \end{pmatrix}, \tag{61}$$

where

$$\mathbf{W}_{i,j} = \mathbf{\Gamma}\Big((||\mathbf{H}_j||^2 + N_o)\mathbf{F}_i^H - \mathbf{R}_{ij}\mathbf{F}_j^H\Big). \tag{62}$$

It is interesting to note that the design matrices associated with the unity rate real orthogonal STBCs for $n_t = 3$ and 4 [48, (37)-(38)], have some unique properties in addition to (10), namely $\mathbf{A}_3\mathbf{A}_1^T = \mathbf{A}_4\mathbf{A}_2^T$ and $\mathbf{A}_3\mathbf{A}_2^T = -\mathbf{A}_4\mathbf{A}_1^T$ [32]. For such OSTBCs, it is not difficult to show that $\mathbf{R}_{12}\mathbf{R}_{12}^T = \alpha\mathbf{I}$, where

$$\alpha = \sum_{k=1}^{4}\big[\mathrm{tr}\big(\mathrm{Re}(\mathbf{H}_1^H\mathbf{H}_2\mathbf{A}_k\mathbf{A}_1^T)\big)\big]^2. \tag{63}$$

It may be noted that the product $\mathbf{A}_k\mathbf{A}_1^T$ is a sparse matrix and hence the computation cost associated with α is very insignificant. On an average, the computation of α involves $n_r n_t$ multiplication operations.

After substituting the simplified expression for $\mathbf{R}_{12}\mathbf{R}_{12}^T$ into (59), the MMSE filter expression in (61) for real orthogonal codes with $n_t = 3$ or 4, can be simplified as

$$\mathbf{W}_{i,j} = \frac{(||\mathbf{H}_j||^2\mathbf{F}_i^H - \mathbf{R}_{ij}\mathbf{F}_j^H)}{(||\mathbf{H}_1||^2 + N_o)(||\mathbf{H}_2||^2 + N_o) - \alpha}, \tag{64}$$

where α is defined as in (63). Now the decoded streams for the two users can be easily obtained as

$$\mathbf{r} = \mathbf{C}\mathbf{y}' = \begin{pmatrix} \mathrm{Re}(\mathbf{W}_{1,2}\mathbf{y}) \\ \mathrm{Re}(\mathbf{W}_{2,1}\mathbf{y}) \end{pmatrix}, \tag{65}$$

where $\mathrm{Re}(\mathbf{W}_{i,j}\mathbf{y})$ corresponds to the decoded stream for the i^{th} user. It may be noted that the expression $\mathbf{W}_{i,j}$ in (64) does not involve any matrix inversion. The computation of $\mathbf{W}_{i,j}$ with the aid of equation (64) only requires $3n_r n_t + 2nn_r n_s^2$ multiplication operations compared to $2n_r n_t + 3nn_r n_s^2 + n_s^2 + n_s^3$ needed if $\mathbf{W}_{i,j}$ is computed using (59) and (62). As a numerical example, for $n_t = 3$ and $n_r = 2$, computation of $\mathbf{W}_{i,j}$ in (62) and (64) requires 274 and 476 multiplication operations, respectively. Thus, the proposed MMSE-based IC of two co-channel users with real STBCs can be achieved using simple linear processing.

In contrast to the presented algorithm, Stamoulis et al. [45] constrain the matrix filter to have identity blocks on the main diagonal and require that the off-diagonals remove all interference:

$$\mathbf{r}_i = \mathbf{y}_i - \mathbf{Z}_i \mathbf{y}_j, \tag{66}$$

where $i, j \in (1, 2)$, $j \neq i$ and $\mathbf{r}_i$ indicates the post-IC recovered data stream corresponding to the i^{th} user. The matrix $\mathbf{Z}_i$ denotes the space-time filter for the i^{th} user as defined in [45, (11)], and $\mathbf{y}_i$ indicates the baseband signal corresponding to the i^{th} receive antenna. In other words, the i^{th} antenna is intended to receive only the i^{th} user; the other antenna is used only to estimate and subtract the interference that is in the i^{th} antenna. While this is a zero-forcing (ZF) solution, it does not have the most general (i.e. full matrix) formulation, and as we will show, it suffers a significant SNR degradation relative to the MMSE solution as well as the full-matrix ZF solution.

6.2 IC with Rate-1/2 Complex OSTBCs

Let us consider two co-channel users, each employing the same rate-1/2 complex orthogonal code. A rate-1/2 generalized complex orthogonal design can be constructed from a real orthogonal design $\mathbf{X}_{n_t}$ as $\mathbf{X}_{n_t}^C = \begin{pmatrix} \mathbf{X}_{n_t} & \text{conj}(\mathbf{X}_{n_t}) \end{pmatrix}$ and can also be represented as

$$\mathbf{X}_{n_t}^C = \sum_{i=1}^{n_s} \text{Re}(s_i) \begin{pmatrix} \mathbf{A}_i & \mathbf{A}_i \end{pmatrix} + j\text{Im}(s_i) \begin{pmatrix} \mathbf{A}_i & -\mathbf{A}_i \end{pmatrix}, \tag{67}$$

where $\mathbf{X}_{n_t}^C$ is the $n_t \times (2n)$ STBC matrix, $\{s_i\}_{i=1}^{n_s}$ denotes the transmitted complex symbols, $\{\mathbf{A_i}\}_{i=1}^{n_s}$ are the $n_t \times n$ matrices representing the code structure of parent real codes, and the operator conj(.) denotes the conjugate of its argument. Following the development similar to (11)-(56), and observing that n_s symbols are transmitted using n_t antennas in $2n$ timeslots, it is not difficult to show that the $2n \times 1$ vector

representing the received baseband signal for the first link can be expressed as

$$\begin{pmatrix} \mathbf{y}_{1:n} \\ \mathbf{y}_{n+1:2n} \end{pmatrix}' = \mathbf{G}'\mathbf{s}' + \mathbf{v}', \tag{68}$$

where $\mathbf{G} = \begin{pmatrix} \mathbf{G}_1 & \mathbf{G}_2 \end{pmatrix}$, and $\mathbf{G}_k$'s are defined as

$$\mathbf{G}_k = \begin{pmatrix} \mathbf{F}_k & j\mathbf{F}_k \\ \mathbf{F}_k & -j\mathbf{F}_k \end{pmatrix}. \tag{69}$$

where the subscript $k \in (1, 2)$. Following the development similar to (56)-(63) and after some simplifications, the linear MMSE detector expression can be shown to be

$$\mathbf{C} = \frac{1}{2}\begin{pmatrix} \mathrm{Re}(\mathbf{W}_{1,2}) & \mathrm{Re}(\mathbf{W}_{1,2}) & -\mathrm{Im}(\mathbf{W}_{1,2}) & -\mathrm{Im}(\mathbf{W}_{1,2}) \\ \mathrm{Im}(\mathbf{W}_{1,2}) & -\mathrm{Im}(\mathbf{W}_{1,2}) & \mathrm{Re}(\mathbf{W}_{1,2}) & -\mathrm{Re}(\mathbf{W}_{1,2}) \\ \mathrm{Re}(\mathbf{W}_{2,1}) & \mathrm{Re}(\mathbf{W}_{2,1}) & -\mathrm{Im}(\mathbf{W}_{2,1}) & -\mathrm{Im}(\mathbf{W}_{2,1}) \\ \mathrm{Im}(\mathbf{W}_{2,1}) & -\mathrm{Im}(\mathbf{W}_{2,1}) & \mathrm{Re}(\mathbf{W}_{2,1}) & -\mathrm{Re}(\mathbf{W}_{2,1}) \end{pmatrix} \tag{70}$$

where $\mathbf{W}_{i,j}$ is defined in (62). After some simplifications, the decoded streams corresponding to the two users can be obtained as

$$\mathbf{r}' = \frac{1}{2}\begin{pmatrix} \mathrm{Re}(\mathbf{W}_{1,2}(\mathbf{y}_{1:n} + \mathbf{y}_{n+1:2n})) \\ \mathrm{Im}(\mathbf{W}_{1,2}(\mathbf{y}_{1:n} - \mathbf{y}_{n+1:2n})) \\ \mathrm{Re}(\mathbf{W}_{2,1}(\mathbf{y}_{1:n} + \mathbf{y}_{n+1:2n})) \\ \mathrm{Im}(\mathbf{W}_{2,1}(\mathbf{y}_{1:n} - \mathbf{y}_{n+1:2n})) \end{pmatrix} \tag{71}$$

or expressed differently as

$$\mathbf{r} = \frac{1}{2}\begin{pmatrix} \mathbf{W}_{1,2}\mathbf{y}_{1:n} + \mathrm{conj}(\mathbf{W}_{1,2}\mathbf{y}_{n+1:2n}) \\ \mathbf{W}_{2,1}\mathbf{y}_{1:n} + \mathrm{conj}(\mathbf{W}_{2,1}\mathbf{y}_{n+1:2n}) \end{pmatrix} \tag{72}$$

The above equation shows that the IC of two co-channel users employing the derived rate-1/2 complex OSTBCs can be implemented using the same MMSE filter designs, $\mathbf{W}_{i,j}$, as for the IC of two users employing real STBCs.

It may be noted that for $n_t = 3$ and 4 there exist higher rate complex OSTBCs than rate-1/2 codes considered in this paper. For example, there exist rate-3/4 codes

called truncated Octonion and Octonion for $n_t = 3$ and 4, respectively [32, (7.4.8)-(7.4.10)]. We further note that the above IC simplification cannot be achieved using these codes as the corresponding matrices $\mathbf{R}_{12}\mathbf{R}_{12}^T$ are not diagonal as required to simplify (59).

6.3 Simulation Examples

Figure 20 shows the average BER performance of the proposed interference suppression technique. The simulation results assume two co-channel users, A and B, each equipped with 3 transmit antennas and employing rate-1/2 complex OSTBC [48, (37)]. All channels are assumed to be i.i.d Rayleigh fading channels. QPSK modulation is used and the receiver is assumed to have 2 antennas.

Fig. 20(a) shows the case where the two users have equal power. We also include the zero-forcing (ZF) solution, which can be obtained from the MMSE solution by setting $N_o = 0$. We observe that Stamoulis' IC technique for two users and two receive antennas delivers about the same ABER performance as if there were only one user and one receive antenna; this is consistent with the results in [4]. On the other hand, both the ZF and MMSE solutions have a significant SNR advantage over the Stamoulis' solution; for example, at ABER = 10^{-3}, the SNR advantage is approximately 3.5 dB. Therefore, although Stamoulis' solution separates the two users, it is not optimal with respect to the MSE criterion as it requires 2-stage receive processing and uses one receive antenna specifically to cancel out the interference from the other user.

Fig. 20(b) shows the case of a 10 dB power imbalance between the users. We see that for the higher-powered user, full matrix ZF results are about the same as in Fig. 20(a), but the MMSE case is about 1 dB better at ABER = 10^{-3}. It is well known that the lower-power user will suffer in a linear multi-user detector, and this is confirmed here for all three cases (the top three curves), although the full-matrix

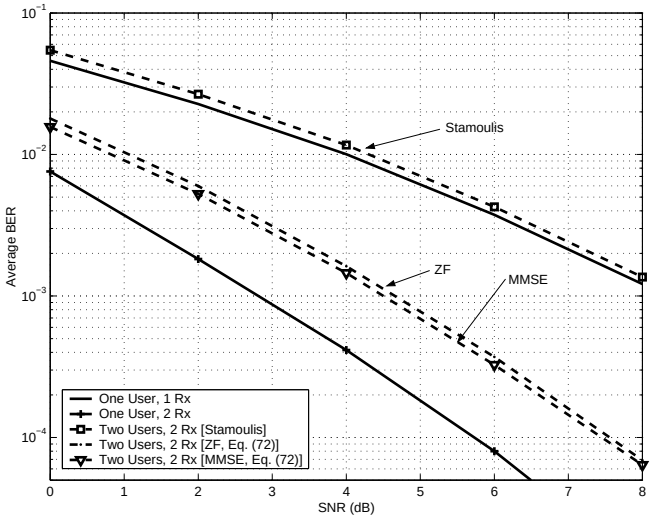

(a) Equi-powered Users, $P_T(A) = P_T(B)$

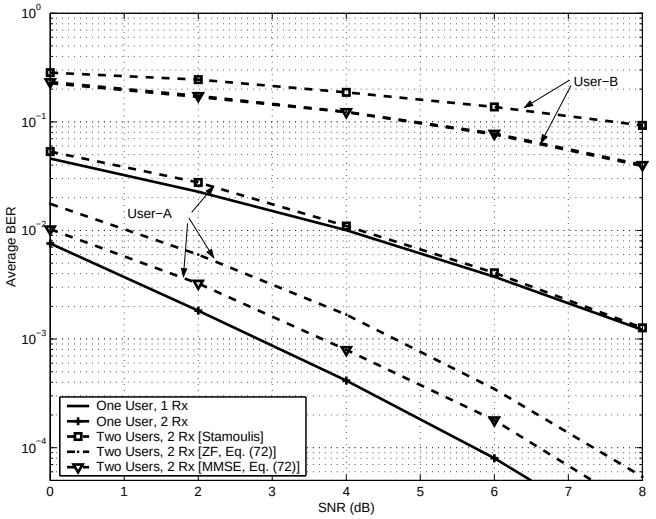

(b) Power imbalance, $P_T(A) = 10P_T(B)$

Figure 20: Average BER performance of User-A

solutions still outperform Stamoulis et al.ś solution.

6.4 Summary

A simple single-stage interference suppression method is proposed that exploits the algebraic structure of unity rate OSTBCs for 3 and 4 transmit antennas. The proposed method provides an MMSE-optimal interference suppression technique that is also low complexity because it avoids matrix inversion. The simulation results show the advantages of the proposed method.

CHAPTER VII

IC OF ALAMOUTI INTERFERENCE FOR A V-BLAST USER

In the previous chapter, we considered the problem of interference cancellation for two co-channel OSTBC users. The analysis presented therein along with the related work in [15, 45, 53, 29, 30] assume that all users employ the same OSTBC. However, in a MIMO network different nodes can transmit using different transmission techniques including V-BLAST, beam-forming or STBC to improve the overall network performance. The BER of a single-input multiple-output (SIMO) or a MIMO link subjected to STBC interference can be significantly improved if the victim receiver exploits the rich algebraic structure of the STBC interference [30, 31]. In [55], Zhang et al. exploit the algebraic properties of Alamouti code to develop a selective co-channel interference mitigation method for two users employing Alamouti codes. In [46], MMSE-based IC is modified to adept to beamforming, which further improves the BER performance.

In [39], Okazaki et al. consider symbol detection problem for a hybrid STBC system that transmits both STBC symbols and Spatial Multiplexing (SM) symbols simultaneously. In such systems, conventional SIC detects STBC symbols first owing to their inherent SNR advantage. As a result, STBC symbols suffer more from residual interference compared to SM symbols, which are detected at a later stage. The authors propose a soft decision SIC which changes detection order at every stage so as to minimize the residual interference faced by each symbol. Different from computationally intensive IC techniques presented in [39], we develop computationally efficient but sub-optimal linear space-time IC techniques, which outperform conventional linear IC techniques that do not take the structure of Alamouti interference

into account.

In the following, we first consider a SIMO link subjected to Alamouti interference and develop IC techniques that exploit the temporal and spatial structure of the Alamouti code. In the subsequent sections, we extend the framework to include a V-BLAST link and present simulation results to evaluate the various aspects of the proposed IC technique. Based on our results, we can make the novel observation that Alamouti interference is less severe than a single-input single-output (SISO) interference.

7.1 System Model

We consider a system comprising two links (pairs of transmit and receive nodes), where each link is subjected to co-channel interference from the other link. The desired link is assumed to have n_t transmit and n_r receive antenna elements whereas the interfering link is assumed to have m_t transmit antenna elements. During each symbol period, n_t input symbols are spatially multiplexed for transmission over the desired link whereas the interfering link transmits space-time block coded symbols. The received baseband vector corresponding to the desired link is given by

$$\mathbf{r} = \sqrt{\rho}\mathbf{H}\mathbf{x} + \sqrt{\mu}\mathbf{G}\mathbf{y} + \mathbf{n} \tag{73}$$

where $\{\mathbf{H},\ \rho\}$ and $\{\mathbf{G},\ \mu\}$ denote the channel gain matrices and noise normalized powers corresponding to the desired and interfering links, respectively. Furthermore, the channel gain matrices are assumed to be slowly varying, Rayleigh faded, and fixed for the duration of an entire burst. The entries of the channel matrices are independent Gaussian distributed complex random variables with zero mean and unit variance. The vectors $\{\mathbf{x}, \mathbf{y}\}$ denote the transmit symbols for the desired and interfering links, respectively. The noise $\mathbf{n}$ is assumed to be additive white Gaussian noise (AWGN) with zero mean and unit variance.

7.2 IC for a SIMO Link

In this section, we focus on the IC of two synchronous co-channel users. The interferer is assumed to be using the Alamouti OSTBC and the desired SIMO link consists of consists of one transmit antenna and two receive antennas. In the following, we present a linear SIMO receiver processor, which exploits the structure of the Alamouti code to separate out the desired symbols.

Let $h_{i,j}$ and $g_{i,j}$ indicate the complex channel gain between the i^{th} receive antenna and j^{th} transmit antenna for the desired and the interfering links, respectively. Now the received baseband vector at the k^{th} receive antenna, r_k^1, can be written as

$$r_k^1 = \sqrt{\rho} h_{k,1} x^1 + \sqrt{\mu} g_{k,1} y_1 + \sqrt{\mu} g_{k,2} y_2 + n_k^1 \tag{74}$$

where the superscript denotes the timeslot index. During the next timeslot, assuming that the channel gains for the desired and the interfering link remain the same, the receive baseband signal r_k^2 can be expressed as

$$r_k^2 = \sqrt{\rho} h_{k,1} x^2 + \sqrt{\mu} g_{k,1} y_2^* - \sqrt{\mu} g_{k,2} y_1^* + n_k^2 \tag{75}$$

The received baseband signal at the k^{th} antenna in (74)-(75) can be represented in matrix notations to facilitate further analysis as

$$\mathbf{r}_k = \begin{pmatrix} r_k^1 \\ r_k^{2*} \end{pmatrix} = \sqrt{\rho} \underbrace{\begin{pmatrix} h_{k,1} & 0 \\ 0 & h_{k,1}^* \end{pmatrix}}_{\mathbf{H}_{k,1}} \underbrace{\begin{pmatrix} x^1 \\ x^{2*} \end{pmatrix}}_{\mathbf{w}} + \sqrt{\mu} \underbrace{\begin{pmatrix} g_{k,1} & g_{k,2} \\ -g_{k,2}^* & g_{k,1}^* \end{pmatrix}}_{\mathbf{G}_k} \underbrace{\begin{pmatrix} y_1 \\ y_2 \end{pmatrix}}_{\mathbf{y}} + \underbrace{\begin{pmatrix} n_k^1 \\ n_k^{2*} \end{pmatrix}}_{\mathbf{n}_k} \tag{76}$$

or

$$\mathbf{r}_k = \sqrt{\rho} \mathbf{H}_{k,1} \mathbf{w} + \sqrt{\mu} \mathbf{G}_k \mathbf{y} + \mathbf{n}_k \tag{77}$$

Using the orthogonality of Alamouti code, viz. $\mathbf{G}_k^H \mathbf{G}_k = \frac{1}{2} ||\mathbf{G}_k||^2 \mathbf{I}$, the interference can be cancelled using the following linear combination of the received baseband vectors as

$$\boldsymbol{\upsilon} = \mathbf{G}_2^H \mathbf{r}_2 / ||\mathbf{G}_2||^2 - \mathbf{G}_1^H \mathbf{r}_1 / ||\mathbf{G}_1||^2 \tag{78}$$

which is equivalent to

$$\boldsymbol{\upsilon} = \sqrt{\rho}\boldsymbol{\Psi}\mathbf{w} + \boldsymbol{\eta} \tag{79}$$

where $\boldsymbol{\Psi} = \mathbf{G}_2^H\mathbf{H}_{2,1}/||\mathbf{G}_2||^2 - \mathbf{G}_1^H\mathbf{H}_{1,1}/||\mathbf{G}_1||^2$, and $\boldsymbol{\eta} = \mathbf{G}_2^H\mathbf{n}_2/||\mathbf{G}_2||^2 - \mathbf{G}_1^H\mathbf{n}_1/||\mathbf{G}_1||^2$ denotes the resultant noise term, which follows the distribution of Additive White Gaussian Noise with zero mean and a variance $(\frac{1}{||\mathbf{G}_1||^2} + \frac{1}{||\mathbf{G}_2||^2})$. It can be easily verified that the matrix $\boldsymbol{\Psi}$ follows the algebraic structure of Alamouti code. Hence, the desired symbols in (79) can be easily decoupled using the matched filter $\boldsymbol{\Psi}^H$ as

$$\widetilde{\boldsymbol{\upsilon}} = \boldsymbol{\Psi}^H\boldsymbol{\upsilon} = \sqrt{\rho}(\boldsymbol{\Psi}^H\boldsymbol{\Psi})\mathbf{w} + \boldsymbol{\Psi}^H\boldsymbol{\eta} \tag{80}$$

where $\boldsymbol{\Psi}^H\boldsymbol{\Psi}$ is a 2×2 diagonal matrix. It is interesting to note that unique structure of $\boldsymbol{\Psi}^H$ implies that the resultant noise term $\boldsymbol{\Psi}^H\boldsymbol{\eta}$ is also AWGN.

7.2.1 Numerical Results

The diversity gain of a system is characterized by the symbol error probability in the high SNR regime. A symbol error occurs when the overall channel gain is smaller than the noise variance, which has a probability $\mathbb{P}\{\gamma < \frac{1}{\rho}\}$. In the high SNR regime, this probability is proportional to ρ^{-D}, where D denotes the diversity gain of the system. Thus the diversity gain of a system may be computed as [50]

$$D = -\lim_{\rho \to \inf} \frac{\mathrm{d}}{\mathrm{d}\ln\rho}[\ln F_\gamma(1/\rho)] \tag{81}$$

where $F_\gamma(.)$ denotes the cumulative density function (CDF) of the normalized SNR γ, which can be obtained from (80) after algebraic manipulations as

$$\gamma = \frac{|h_{1,1}|^2\sum_{i=1}^{2}|g_{i,2}|^2 + |h_{2,1}|^2\sum_{i=1}^{2}|g_{i,1}|^2 - 2Re(g_{1,1}^*h_{1,1}h_{2,1}^*g_{1,2} + g_{2,1}h_{1,1}^*h_{2,1}g_{2,2}^*)}{\sum_{i=1}^{2}(|g_{i,1}|^2 + |g_{i,2}|^2)} \tag{82}$$

Unfortunately, a closed-form expression for $F_\gamma(\gamma)$ appears difficult to obtain. We, therefore, resort to Monte Carlo simulation for generating the CDF. Figure 21 shows

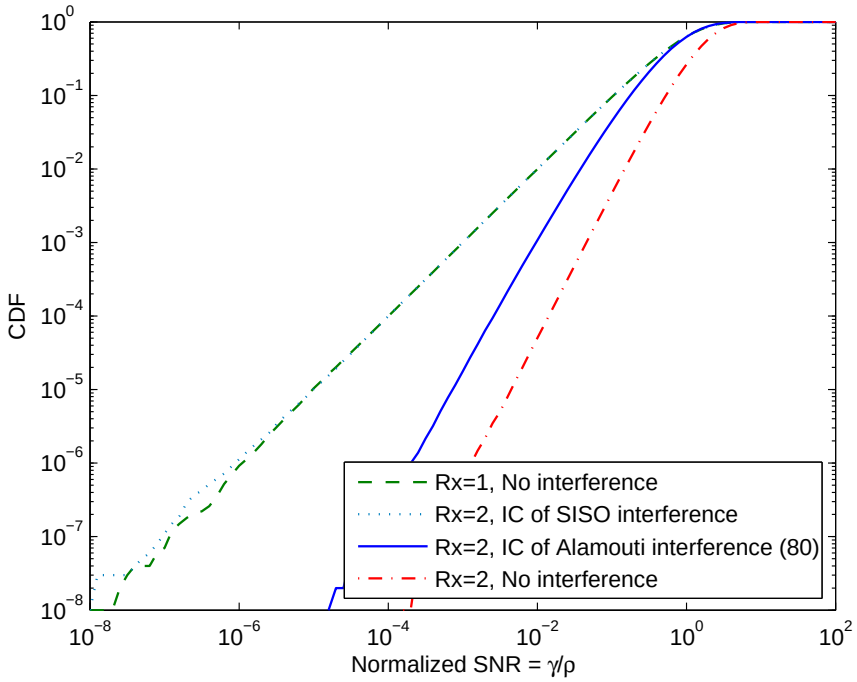

Figure 21: The cumulative density function of normalized SNR for various interference scenarios with SIR = 0dB.

the numerical $F_\gamma(\gamma)$ computed using 10^7 channel trials as a function of γ. A logarithmic XY scale is chosen so that the diversity order can be reflected by the slope of respective CDF tails. It is not difficult to observe from Figure 21 that the slope of CDF tails for *no interference* scenarios with 1 and 2 receive antennas is approximately 1 and 2, respectively. Therefore, the diversity order of these two scenarios is 1 and 2, respectively, as expected. Next, we observe from the slope of CDF tail of the expression in (82) that the diversity order of the concerned system is closer to 2. However, it must be noted that this diversity gain is fully realized at much higher SNR compared to the scenario with no interference and 2 receive antennas. On the other hand, the scenario with single-input single output (SISO) interference and 2 receive antennas perform the same as a SISO link with no interference.

For a more practical comparison, Figure 22 shows the comparative BER performance for the same scenario as in Figure 21. All transmitters are equi-powered and

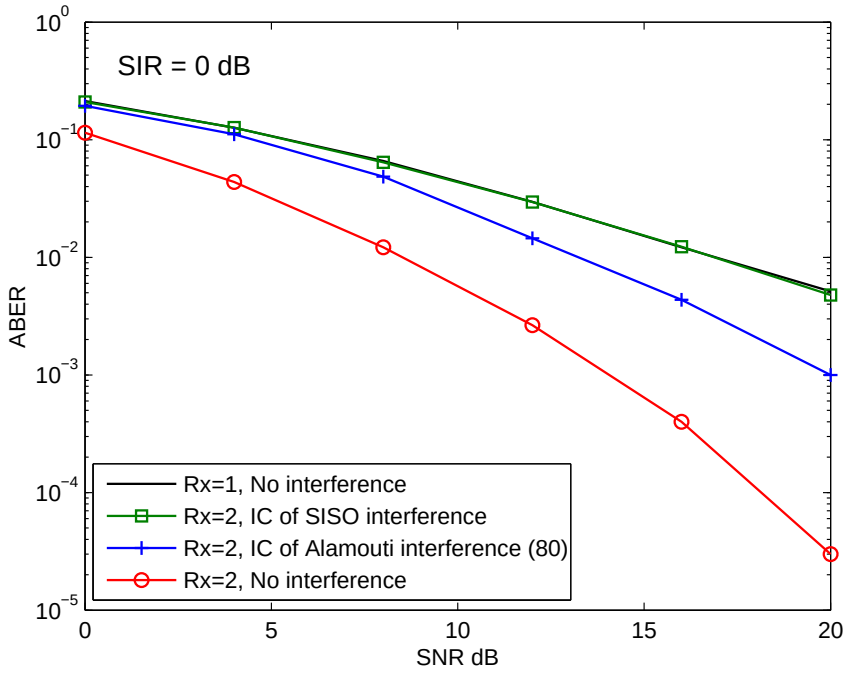

Figure 22: Average bit error probability as a function of SNR with SIR = 0dB.

employ QPSK modulation. The results are generated using Monte Carlo simulation of 10^7 channel trials. It is apparent that a SIMO link subjected to Alamouti interference performs better than the SIMO link subjected to SISO interference. Also, the gap between the BER curves for SISO and SIMO link with Alamouti interference increases with increasing SNR, which is indicative of its higher diversity gain as reflected in Figure 21.

7.3 IC for a V-BLAST Link

In the previous section, we treated the case where the desired signal was transmitted by a single antenna (i.e. the link was SIMO), and the interference was STBC. In this section, we extend the analysis to include a V-BLAST link subjected to Alamouti interference from another co-channel user.

Following the development in the previous section, the received baseband signal

at k^{th} receive antenna can be expressed as:

$$\mathbf{r}_k = \begin{pmatrix} r_k^1 \\ r_k^{2*} \end{pmatrix} = \sqrt{\rho} \begin{pmatrix} \mathbf{h}_k & \mathbf{0} \\ \mathbf{0} & \mathbf{h}_k^* \end{pmatrix} \begin{pmatrix} \mathbf{x}^1 \\ \mathbf{x}^{2*} \end{pmatrix} + \sqrt{\mu} \begin{pmatrix} g_{k,1} & g_{k,2} \\ -g_{k,2}^* & g_{k,1}^* \end{pmatrix} \begin{pmatrix} y_1 \\ y_2 \end{pmatrix} + \begin{pmatrix} n_k^1 \\ n_k^{2*} \end{pmatrix} \quad (83)$$

where $\mathbf{h}_k = \begin{pmatrix} h_{k,1} \cdots h_{k,n_t} \end{pmatrix}$ denotes the k^{th} row vector of the corresponding channel matrix $\mathbf{H}$, $\mathbf{x}$ denotes the transmitted vector, and the superscripts denote the associated timeslot index. The rest of the variables follow the same definition as in the previous section. The received baseband vector in (83) can be rewritten to better exploit the structure of Alamouti code as

$$\mathbf{r}_k = \sqrt{\rho} \begin{pmatrix} \mathbf{H}_{k,1} \cdots \mathbf{H}_{k,n_t} \end{pmatrix} \begin{pmatrix} \mathbf{w}_1 \\ \vdots \\ \mathbf{w}_{n_t} \end{pmatrix} + \sqrt{\mu} \mathbf{G}_k \mathbf{y} + \mathbf{n}_k \quad (84)$$

where, $\mathbf{w}_j$ denotes the 2×1 vector comprising the desired symbols transmitted by the j^{th} antenna during the two consecutive timeslots, i.e.,

$$\mathbf{w}_j = \begin{pmatrix} x_j^1 \\ x_j^{2*} \end{pmatrix} \quad (85)$$

and $\mathbf{H}_{k,j}$ is defined as

$$\mathbf{H}_{k,j} = \begin{pmatrix} h_{k,j} & 0 \\ 0 & h_{k,j}^* \end{pmatrix} \quad (86)$$

Now the desired symbols can be recovered employing the zero-forcing (ZF) based linear block filter given by

$$\mathbf{Z} = \text{pinv} \begin{pmatrix} \mathbf{H}_{1,1} & \cdots & \mathbf{H}_{1,n_t} & \mathbf{G}_1 \\ \mathbf{H}_{2,1} & \cdots & \mathbf{H}_{2,n_t} & \mathbf{G}_2 \\ \vdots & \ddots & \vdots & \vdots \\ \mathbf{H}_{n_r,1} & \cdots & \mathbf{H}_{n_r,n_t} & \mathbf{G}_{n_r} \end{pmatrix} \quad (87)$$

where pinv denotes the Moore-Penrose pseudoinverse. It is apparent that the numerical complexity of computing $\mathbf{Z}$ can be prohibitive with increasing number of receive

and/or transmit antennas. We, therefore, look into sub-optimal ways of recovering the desired symbols.

7.3.1 Sub-optimal IC

The received baseband signal at the n^{th} receive antenna can be employed to cancel out the Alamouti interference at other receive antennas using the following linear combination,

$$\boldsymbol{\upsilon}_k = \mathbf{G}_k^H \mathbf{r}_k / ||\mathbf{G}_k||^2 - \mathbf{G}_n^H \mathbf{r}_n / ||\mathbf{G}_n||^2 \tag{88}$$

Without loss of generality, let's assume that 1^{st} receive antenna is used to cancel out the Alamouti interference, i.e. $n = 1$. Now the interference-free vectors, $\boldsymbol{\upsilon}_k$, can be stacked together to obtain the following representation

$$\boldsymbol{\upsilon} = \begin{pmatrix} \boldsymbol{\upsilon}_2 \\ \boldsymbol{\upsilon}_3 \\ \vdots \\ \boldsymbol{\upsilon}_{n_r} \end{pmatrix} = \sqrt{\rho} \underbrace{\begin{pmatrix} \boldsymbol{\Psi}_{2,1} & \boldsymbol{\Psi}_{2,2} & \cdots & \boldsymbol{\Psi}_{2,n_t} \\ \boldsymbol{\Psi}_{3,1} & \boldsymbol{\Psi}_{3,2} & \cdots & \boldsymbol{\Psi}_{3,n_t} \\ \vdots & \vdots & \ddots & \vdots \\ \boldsymbol{\Psi}_{n_r,1} & \boldsymbol{\Psi}_{n_r,2} & \cdots & \boldsymbol{\Psi}_{n_r,n_t} \end{pmatrix}}_{\boldsymbol{\Psi}} \underbrace{\begin{pmatrix} \mathbf{w}_1 \\ \mathbf{w}_2 \\ \vdots \\ \mathbf{w}_{n_t} \end{pmatrix}}_{\mathbf{w}} + \underbrace{\begin{pmatrix} \boldsymbol{\eta}_2 \\ \boldsymbol{\eta}_3 \\ \vdots \\ \boldsymbol{\eta}_{n_r} \end{pmatrix}}_{\boldsymbol{\eta}} \tag{89}$$

or

$$\boldsymbol{\upsilon} = \sqrt{\rho} \boldsymbol{\Psi} \mathbf{w} + \boldsymbol{\eta} \tag{90}$$

where the 2×2 sub-matrices $\boldsymbol{\Psi}_{k,j}$ are given by

$$\boldsymbol{\Psi}_{k,j} = \mathbf{G}_k^H \mathbf{H}_{k,j} / ||\mathbf{G}_k||^2 - \mathbf{G}_1^H \mathbf{H}_{1,j} / ||\mathbf{G}_1||^2 \tag{91}$$

and the resultant noise components $\boldsymbol{\eta}_k$ are given by

$$\boldsymbol{\eta}_k = \mathbf{G}_k^H \mathbf{n}_k / ||\mathbf{G}_k||^2 - \mathbf{G}_1^H \mathbf{n}_1 / ||\mathbf{G}_1||^2 \tag{92}$$

Again, it can be easily verified that the sub matrices $\boldsymbol{\Psi}_{k,j}$ follow the algebraic structure of Alamouti code, i.e. the product $\boldsymbol{\Psi}_{k,j}^H \boldsymbol{\Psi}_{k,j}$ is a diagonal matrix. Unfortunately, the

said property doesn't hold for $\mathbf{\Psi}$ as $\mathbf{\Psi}^H\mathbf{\Psi}$ is not diagonal if $n_t > 1$. Therefore, the symbol decoupling in a V-BLAST link is more involved compared to a SIMO link.

Since only one additional receive antenna is used to suppress Alamouti interference, we need $n_r \geq n_t + 1$. For the following analysis, let us assume $n_r = n_t + 1$. Now, to recover the transmitted symbols, we follow the approach similar to [45] and partition the matrix $\mathbf{\Psi}$ into four blocks as

$$\mathbf{\Psi} = \begin{pmatrix} \mathbf{\Psi}_{2,1} & \mathbf{B} \\ \mathbf{C} & \mathbf{D} \end{pmatrix} \tag{93}$$

where $\mathbf{B}$, $\mathbf{C}$, and $\mathbf{D}$ denote the $2 \times 2(n_t - 1)$ upper-right, $2(n_t - 1) \times 2$ lower-left and $2(n_1 - 1) \times 2(n_t - 1)$ lower-right submatrices of $\mathbf{\Psi}$. Now, to recover the transmitted symbols from the 1^{st} antenna during the two timeslots, we design the following block linear filter

$$\mathbf{\Phi} = \begin{pmatrix} \mathbf{I}_2 & -\mathbf{B}\mathbf{D}^{-1} \\ -\mathbf{C}\mathbf{\Psi}_{2,1}^{-1} & \mathbf{I}_{2n_t-2} \end{pmatrix} \tag{94}$$

which when applied to $\boldsymbol{\upsilon}$ in (90) gives

$$\begin{pmatrix} \widetilde{\boldsymbol{\upsilon}}_1 \\ \boldsymbol{\upsilon}_{n_t-1} \end{pmatrix} = \sqrt{\rho} \begin{pmatrix} (\mathbf{\Psi}_{2,1} - \mathbf{B}\mathbf{D}^{-1}\mathbf{C})\mathbf{w}_1 \\ (\mathbf{D} - \mathbf{C}\mathbf{\Psi}_{2,1}^{-1}\mathbf{B})\mathbf{w}_{(n_t-1)} \end{pmatrix} + \mathbf{\Phi}\boldsymbol{\eta} \tag{95}$$

where $\mathbf{w}_{(n_t-1)}$ denotes the lower $(n_t - 1)$ subvectors of $\mathbf{w}$, which will be used for the recovery of the symbols transmitted from other antennas, whereas the symbols corresponding to the first antenna will be recovered from $\widetilde{\boldsymbol{\upsilon}}_1$. Furthermore, we can iteratively apply the same procedure to $\mathbf{w}_{(n_t-1)}$ to recover the symbols transmitted from the remaining $n_t - 1$ antennas. For example, the transmitted vectors for a 2×3 V-BLAST link can be recovered using (95) as

$$\begin{pmatrix} \widetilde{\boldsymbol{\upsilon}}_1 \\ \widetilde{\boldsymbol{\upsilon}}_2 \end{pmatrix} = \sqrt{\rho} \begin{pmatrix} (\mathbf{\Psi}_{2,1} - \mathbf{\Psi}_{2,2}\mathbf{\Psi}_{3,2}^{-1}\mathbf{\Psi}_{3,1})\mathbf{w}_1 \\ (\mathbf{\Psi}_{3,2} - \mathbf{\Psi}_{3,1}\mathbf{\Psi}_{2,1}^{-1}\mathbf{\Psi}_{2,2})\mathbf{w}_2 \end{pmatrix} + \mathbf{\Phi}\boldsymbol{\eta} \tag{96}$$

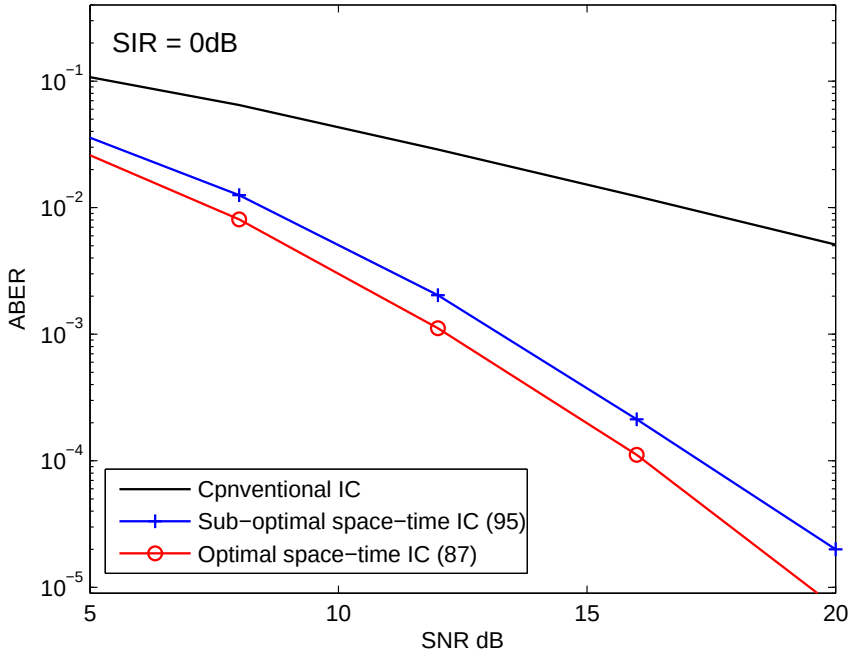

Figure 23: Average bit error probability for 2×4 V-BLAST link in presence of Alamouti interferer with SIR = 0dB.

7.3.2 Numerical Results

Figure 23 shows the average BER performance of 2×4 V-BLAST link employing various IC techniques for suppressing Alamouti interference. All transmitters are equi-powered and employ QPSK modulation. The results are generated using Monte Carlo simulation of 10^7 channel trials. The conventional IC technique does not take the structure of Alamouti interference into account and as a result it perceives Alamouti interference as comprising of two independent data streams. As a result, conventional IC techniques gives far inferior BER performance when compared to the other two space-time IC techniques, which exploit the time-correlation in interference data streams. It is apparent that space-time IC techniques in Figure 23 offer higher diversity order compared to conventional IC technique. The optimal space-time IC technique in (87) offers a gain of about 1 dB over sub-optimal IC technique presented in (95) at much higher computation cost.

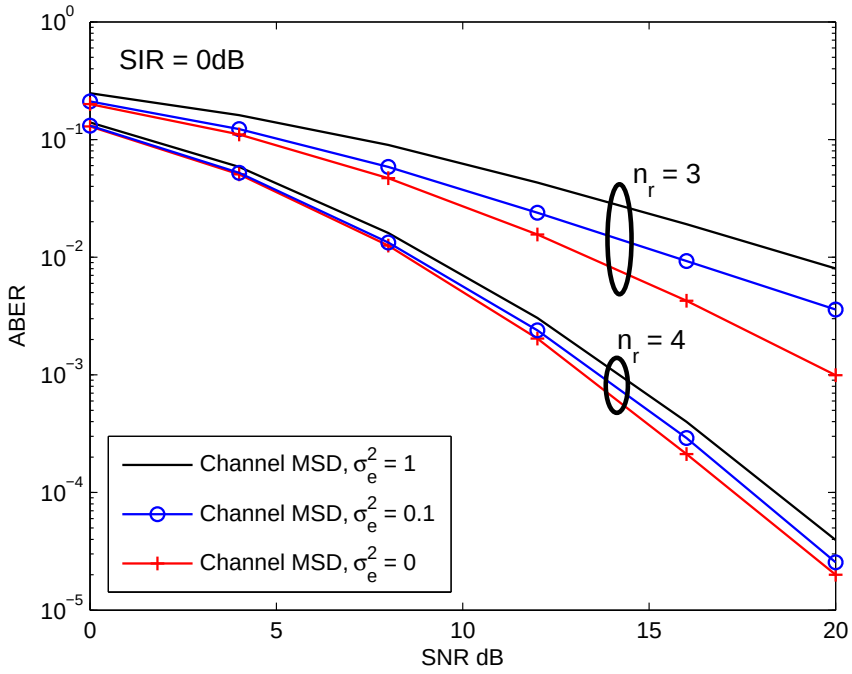

Figure 24: Average bit error probability with varying mean squared deviation (MSD) in channel during consecutive timeslots.

The results presented in this chapter assume that the channel for the V-BLAST link remains unchanged for the duration of two timeslots over which Alamouti interference is encoded. In Figure 24, we investigate the impact of V-BLAST channel deviation on its BER performance assuming QPSK modulation. The mean standard deviation (MSD) in consecutive channel gain matrices is measured as

$$\sigma_e = \sqrt{\frac{1}{n_r \times n_t} \mathrm{E}\big(||\mathbf{H}_1|| - ||\mathbf{H}_2||\big)^2} \tag{97}$$

From Figure 24, we note that for a 2×3 V-BLAST link, the deviation in channel affects the link BER quite adversely. For example, to achieve an average BER $= 10^{-2}$, an MSD $= 0.1$ results in 2.3 dB SNR penalty whereas, an MSD $= 1$ causes 5.6 dB SNR penalty. However, when an additional receive antenna is employed, the corresponding SNR penalties dramatically drop down to 0.15 and 0.65 dB, respectively. This implies that the proposed space-time IC techniques can still be effective when the channel MSD is higher as long as sufficient number of receive antennas are employed.

7.4 Summary

In this chapter, we have developed sub-optimal space-time IC techniques for a V-BLAST link subjected to Alamouti interference. The proposed IC techniques outperform conventional IC techniques that do not take the structure of OSTBC interference into account. Our results also show that the BER of the V-BLAST link depends on the amount of mean-squared deviation in its channel for the duration over which an Alamouti block encoded interference is transmitted. Although the BER performance of V-BLAST link degrades rapidly with increasing channel deviation, employing sufficiently large number of receive antennas can counter the BER degradation due to increasing channel deviation.

CHAPTER VIII

SUMMARY AND FUTURE WORK

In the following, we summarize the primary research contributions and suggested directions for the future work.

8.1 Research Summary

The research reported in this dissertation has looked into the challenges posed by co-channel interference in MIMO networks and provided practical means of managing interference at a marginal cost of system performance.

We have addressed the interference problems arising in the context of SDMA based MIMO networks, which more effectively exploit the available network resources than TDMA based MIMO networks. Sub-optimal techniques for joint optimization of co-channel MIMO links were developed by applying optimal antenna selection aided stream control algorithms. These algorithms were tested on both simulated and measured indoor MIMO channels. We also extended the analysis to investigate the impact of stream control on the performance of interfering MIMO links assuming M-QAM constellations and linear MMSE receiver processor. It was shown that the use of SDMA scheme along with partial CSI (subset of best antennas) at the transmitters significantly reduces the signaling overhead with minimal loss in throughput performance.

The main challenge in employing stream control with optimal antenna selection for OL-SDMA systems is the search of optimal subset of transmit antennas. Towards this, we developed an MSE-based antenna selection framework for implementing low complexity algorithms for finite complexity receivers operating in the presence of co-channel interference. For either the transmitter or receiver antenna selection, two

sequential greedy algorithms were developed, one that starts with a full set of antennas and decrements, and the other that starts with an empty set that increments. The choice of which is best depends on how many antennas will ultimately be selected. These selection algorithms were shown to provide reasonable BER performance while keeping the overall system complexity low.

Next, we addressed the interference problems for space-time encoded transmissions which can be mitigated using only one additional antenna without sacrificing space-time diversity gains. These algebraic properties of linear OSTBCs were exploited to facilitate a single-stage and MMSE optimal detector for two co-channel users employing unity rate real and derived rate-1/2 complex OSTBCs for 3 and 4 transmit antennas. Furthermore, a single-stage multi-user interference suppression technique is proposed for OSTBC interference; this technique exploits the temporal and spatial structure of OSTBCs leading to simple linear processing.

8.2 Suggestions for Future Work

The goal of the reported research is to develop reliable techniques for managing co-channel interference in MIMO networks and jointly optimizing network throughput. Some directions for research to follow the work presented herein are:

- **Finer tradeoff between throughput gain and CSI overhead:** The CSI feedback creates a major overhead for CL-SDMA systems which provide optimal network throughput. However, the computational and signalling complexity associated with CL-SDMA is prohibitive. The proposed OL-SDMA with optimal selection provides a rough tradeoff between network throughput and system complexity. New SDMA techniques based on partial CSI such as second order channel statics can allow finer trade-off.

- **Algorithms for nonlinear receiver architecture:** The stream control algorithms as well as antenna selection algorithms presented in this thesis are

limited to linear receiver processing. However, the use of non-linear processing techniques such as successive interference cancellation (SIC) can improve the BER performance of MIMO links.

- **IC using the interference power covariance matrix:** The IC techniques presented in this dissertation assume the availability of interferer's channel. However, such an assumption is well suited only for multiuser detection. New IC techniques are required which exploit the algebraic structure of power covariance matrix associated with the space-time interference.

- **Design of Cross-layer PHY/MAC protocols:** The sub-optimal MIMO-SDMA algorithms introduced in this dissertation allow multiple co-channel MIMO links to operate simultaneously with higher throughput than with time-multiplexing schemes. However, for users with correlated channels time-multiplexing is preferable. New cross-layer PHY/MAC protocols are needed to facilitate this kind of operation.

- **Rician and Frequency selective channels:** This dissertation addressed only the quasi-static flat fading Rayleigh channel. However, in many situations the line-of-sight (LOS) signal component is also significant resulting in Rician fading channel. The algorithms presented in this thesis can be analyzed for Rician channel and extended to include frequency selective channels which form the basis on many standards including IEEE 802.11n, 802.16e etc.

REFERENCES

[1] Alamouti, S. M., "A simple transmit diversity technique for wireless communications," *IEEE J. Select. Areas Commun.*, vol. 16, pp. 1451–1458, Oct. 1998.

[2] Barry, J. R., Lee, E. A., and Messerschmitt, D. G., *Digital Communications*. Kluwer Academy Publishers, third ed., 2003.

[3] Berenguer, I. and Wang, X., "Mimo antenna selection with lattice reduction aided linear receivers," *IEEE Trans. Vehicular Tech.*, vol. 53, pp. 1289–1302, Sept. 2004.

[4] Berenguer, I., Wang, X., and Wassell, I. J., "Transmit antenna selection in linear receivers: Geometrical approach," *IEE Electronic Letters*, vol. 40, pp. 292–293, Mar. 2004.

[5] Bliss, D., Forsythe, K. W., Hero, A. O., and Yegulalp, A. F., "Environmental issues for mimo capacity," *IEEE Trans. Signal Processing*, vol. 50, pp. 2128–2142, Sept. 2002.

[6] Blum, R. S., "Mimo capacity with interference," *IEEE J. Select. Areas Commun.*, vol. 21, pp. 793–801, June 2003.

[7] Blum, R. S., Winters, J. H., and Sollenberger, N. R., "On the capacity of cellular systems with mimo," *IEEE Communication Letters*, vol. 6, pp. 242–244, June 2002.

[8] Chang, J.-H., Tassiulas, L., and Rashid-Farrokhi, F., "Joint transmitter receiver diversity for efficient space division multiaccess," *IEEE Transactions on Wireless Communications*, vol. 1, pp. 16–27, Jan 2002.

[9] Cho, K. and Yoon, D., "On the general ber expression of one- and two-dimensional amplitude modulations," *IEEE Trans. Commun.*, vol. 50, pp. 1074–1080, July 2002.

[10] Chung, S. T., Lozano, A., and Huang, H. C., "Approaching eigenmode BLAST channel capacity using V-BLAST with rate and power feedback," *Proc. of the IEEE Vehicular Technology Conference*, vol. 2, 2001.

[11] Demirkol, M. F. and Ingram, M. A., "Power-controlled capacity for interfering mimo links," *IEEE Vehicular Technology Conference*, vol. 1, pp. 187–191, Oct. 2001.

[12] Demirkol, M. F. and Ingram, M. A., "Control using capacity constraints for interfering mimo links," *IEEE Int. Symp. on Personal, Indoor, and Mobile Radio Communications*, vol. 3, pp. 1032–1036, Sept. 2002.

[13] Demirkol, M. F. and Ingram, M. A., "Stream control in networks with interfering mimo links," *IEEE Wireless Communications and Networking*, vol. 1, pp. 343–348, Mar. 2003.

[14] Demirkol, M. F., *Resource Allocation for Interfering MIMO Links*. Atlanta, GA: Ph.D Thesis, Georgia Institute of Technology, 2003.

[15] Diggavi, S. N., Al-Dhahir, N., and Calderbank, A. R., "Algebraic properties of space-time block codes in intersymbol interference multiple-access channels," *IEEE Trans. Inform. Theory*, vol. 49, pp. 2403–2414, Oct. 2003.

[16] Farrokhi, F. R., Liu, K. J. R., and Tassiulas, L., "Transmit beamforming and power control for cellular wireless systems," *IEEE J. Select. Areas Commun.*, vol. 16, pp. 1437–1450, Oct. 1998.

[17] Foschini, G. J. and Miljanic, Z., "A simple distributed autonomous power control algorithm and its convergence," *IEEE Trans. Vehicular Tech.*, vol. 42, pp. 641–646, Nov. 1993.

[18] Foschini, G. and Gans, M., "On the limits of wireless communications in a fading environment when using multiple antennas," *Wireless Personal Communicatios*, vol. 6, pp. 311–335, Mar. 1998.

[19] Gharavi-Alkhansari, M. and Gershman, A. B., "Fast antenna subset selection in mimo systems," *IEEE Trans. Signal Processing*, vol. 52, pp. 339–347, Feb. 2004.

[20] Gore, D., Gorokhov, A., and Paulraj, A., "Joint mmse versus v-blast and antenna selection," in *Proc. Asilomar Conference on Signals, Systems and Computers*, vol. 1, pp. 505–509, Nov. 2002.

[21] Gore, D. A., Heath, R. W., and Paulraj, A., "Transmit selection in spatial multiplexing systems," *IEEE Communications Letters*, vol. 6, pp. 491–493, Nov. 2002.

[22] Gorokhov, A., "Antenna selection algorithms for mea transmission systems," in *Proc. IEEE ICASSP*, pp. 2857–2860, May 2002.

[23] Gorokhov, A., Collados, M., Gore, D., and Paulraj, A., "Transmit/receive mimo antenna selection," in *Proc. IEEE ICASSP*, vol. 2, pp. 13–16, May 2004.

[24] Gorokhov, A., Gore, D. A., and Paulraj, A. J., "Receive antenna selection for mimo flat-fading channels: Theory and algorithms," *IEEE Trans. Inform. Theory*, vol. 49, pp. 2667–2696, Oct. 2003.

[25] Heath, R. and Love, D., "Multimode antenna selection for spatial multiplexing systems with linear receivers," *IEEE Trans. Signal Processing*, vol. 53, pp. 3042–3056, Aug. 2005.

[26] Jafarkhani, H., "A quasi-orthogonal space-time block code," *IEEE Trans. Commun.*, vol. 49, pp. 1–4, Jan. 2001.

[27] Jensen, M. and Morris, M., "Efficient capacity-based antenna selection for mimo systems," *IEEE Trans. Vehicular Tech.*, vol. 54, pp. 110–116, Jan. 2005.

[28] Jiang, J.-S. and Ingram, M., "Comparison of beam selection and antenna selection techniques in indoor mimo systems at 5.8 ghz," in *Proc. of Radio and Wireless Conference*, pp. 179–182, Aug. 2003.

[29] Kazemitabar, J. and Jafarkhani, H., "Multiuser interference cancellation and detection for users with four transmit antennas," in *IEEE International Symposium of Information Theory, ISIT*, pp. 1914–1918, 2006.

[30] Klang, G. and Ottersten, B., "Space-time interference rejection cancellation in transmit diversity systems," *The 5th International Conference on Wireless Personal Multimedia Communications*, vol. 2, pp. 706–710, Oct. 2002.

[31] Klang, G., *On Interference Rejection in Wireless Multichannel Systems*. Stockholm, Sweden: Ph.D Thesis, Royal Institute of Technology, 2003.

[32] Larsson, E. G. and Stoica, P., *Space-Time Block Coding for Wireless Communications*. Cambridge, UK: Cambridge University Press, 2003.

[33] Lin, D., Sfar, S., and Letaief, K. B., "Receive antenna selection for mimo systems in correlated channels," in *Proc. IEEE International Conf. on Comm*, vol. 5, pp. 2944–2948, June 2004.

[34] Lotkepohl, H., *Handbook of Matrices*. New York: Wiley, 1996.

[35] Molisch, A., Win, M., and Winters, J., "Capacity of mimo systems with antenna selection," in *Proc. IEEE Int. Conf. Commun. (ICC'01)*, (Helsinki, Finland), pp. 570–574, June 2001.

[36] Nabar, R., Gore, D., and Paulraj, A., "Optimal selection and use of transmit antennas in wireless systems," in *Proc. International Conference on Telecommunications (ICT'00)*, (Acapulco, Mexico), May 2000.

[37] Naguib, A. F., Seshadri, N., and Calderbank, A. R., "Applications of space-time block codes and interference suppression for high capacity and high data rate wireless systems," in *Proc. 32nd Asilomar Conf. Signals, Syst., Comput.*, pp. 1803–1810, 1998.

[38] Nam, S. H. and Lee, K. B., "Transmit power allocation for an extended V-BLAST system," *Proc. of the IEEE Int. Symp. on Personal, Indoor and Mobile Radio Communications*, sep 2002.

[39] Okazaki, A., Fujikawa, M., Hasegawa, K., and Sasase, I., "Soft decision iterative v-blast with detection of all symbols at the last stage by changing detection order in hybrid stbc," in *Proc. IEEE Pacific Rim Conference on Communications, Computers and Signal Processing*, pp. 194–197, Aug. 2007.

[40] Park, J. and Park, D., "A new antenna selection algorithm with low complexity for mimo wireless systems," in *IEEE International Conference on Communications (ICC'2005)*, vol. 4, p. 2308, May 2005.

[41] Runhua, C., Andews, J., and Health, R., "Multiuser space-time block coded mimo with downlink precoding," *IEEE International Conference on Communications*, vol. 5, pp. 2689–2693, June 2004.

[42] Sampath, H., Stoica, P., and Paulraj, A., "Generalized linear precoder and decoder design for mimo channels using the weighted mmse criterion," *IEEE Trans. Commun.*, vol. 49, pp. 2198–2206, Dec. 2001.

[43] Sanayei, G. S., "Antenna selection in mimo systems," *IEEE Commun. Mag.*, vol. 42, pp. 68–73, Oct. 2004.

[44] Sandhu, S., Nabar, R. U., Gore, D. A., and Paulraj, A., "Selecting an optimal set of transmit antennas for a mimo channel based on shannon capacity," in *Proc. Asilomar Conf. Signals, Syst., Comput.*, (Pacific Grove, CA), pp. 567–571, Nov. 2000.

[45] Stamoulis, A., Al-Dhahir, N., and Calderbank, A. R., "Further results on interference cancellation and space-time block codes," in *Proc. Asilomar Conf. Signals, Syst., Comput.*, pp. 257–262, Oct. 2001.

[46] Sun, C. and Karmakar, N. C., "Combining beamforming with mmse alamouti multiuser interference cancellation receiver," in *Proc. Fourth IEEE International Symposium on Signal Processing and Information Technology*, pp. 254–257, Dec. 2004.

[47] Sundaresan, K., Sivakumar, R., Ingram, M. A., and Chang, T.-Y., "A fair medium access control protocol for ad-hoc networks with mimo links," *IEEE Trans. Mobile Comput.*, vol. 3, pp. 350–365, Dec. 2004.

[48] Tarokh, V., Jafarkhani, H., and Calderbank, A. R., "Space-time block codes from orthogonal designs," *IEEE Trans. Inform. Theory*, vol. 45, pp. 1456–1467, July 1999.

[49] Telatar, I., "Capacity of multi-antenna gaussian channels," *AT&T Bell Labs, Technical Report*, pp. 311–335, June 1995.

[50] Tse, D. and Viswanath, P., *Fundamentals of Wireless Communication*. New York: Cambridge University Press, 2005.

[51] Winters, J. H., Salz, J., and Gitlin, R. D., "The impact of antenna diversity on the capacity of wireless communication systems," *IEEE Trans. Commun.*, vol. 42, pp. 1740–1751, Feb./Mar./Apr. 1994.

[52] Wolniansky, P. W., Foschini, G. J., Golden, G. D., and Valenzuela, R. A., "V-blast: an architecture for realizing very high data rates over the rich-scattering wireless channel," *URSI International Symposium on Signals, Systems, and Electronics*, pp. 295–300, Sept. 1998.

[53] Younis, W. M., Sayed, A. H., and Al-Dhahir, N., "Efficient adaptive receivers for joint equalization and interference cancellation in multiuser space-time block-coded systems," *IEEE Trans. Signal Processing*, vol. 51, pp. 2849–2862, Nov. 2003.

[54] Zhang, H., Dai, H., and Zhou, Q., "A geometrical analysis on transmit antenna selection for spatial multiplexing systems with linear receivers," in *Proc. International Symposium on Information Theory*, pp. 1558–1562, Sept. 2005.

[55] Zhang, L., Li, S., Zheng, H., and Wu, M., "A selective co-channel interference mitigation method for alamouti code," in *Proc. 11th IEEE Symposium on Computers and Communications*, pp. 149–154, June 2006.

[56] Zheng, L. and Tse, D., "Diversity and multiplexing: a fundamental tradeoff in multiple-antenna channels," *IEEE Transactions on Information Theory*, vol. 49, pp. 1073–1096, may 2003.

VITA

Sudhanshu Gaur was born in 1979 in Meerut, India. He received Bachelor of Technology degree in Instrumentation Engineering from Indian Institute of Technology, Kharagpur in 2000. Afterwards, he worked with the 2.5G Communications Group of Sasken Communication Technologies, Bangalore. In Fall 2001, he joined the Mobile and Portable Radio Research Group (MPRG) at Virginia Tech for graduate studies. After completing his M.S. in Electrical Engineering in Fall 2003, he joined the Smart Antenna Research Laboratory (SARL) at Georgia Tech to pursue his PhD. In Fall 2005, he joined the Wireless Systems Research Laboratory (WSRL) at Hitachi. His research interests include MIMO signal processing, space-time coding, interference management, resource allocation, random processes and number theory.